# Dietary sodium induces a redistribution of the tubular metabolic workload

Udwan, Khalil ; Abed, Ahmed ; Roth, Isabelle ; Dizin, Eva ; Maillard, Marc ; Bettoni, Carla ; Loffing, Johannes ; Wagner, Carsten A ; Edwards, Aurélie ; Feraille, Eric

Abstract: Na+ excretion by the kidney varies according to dietary Na+ intake. We undertook a systematic study on the effects of dietary salt intake on glomerular filtration rate (GFR) and tubular Na+ reabsorption. We examined the renal adaptive response in mice subjected to 7 days of a low sodium diet (LSD) containing 0.01% Na+ , a normal sodium diet (NSD) containing 0.18% Na+ , as well as a moderately high sodium diet (HSD) containing 1.25% Na+ . As expected, LSD did not alter measured GFR and increased the abundance of total and cell-surface NHE3, NKCC2, NCC, -ENaC, and cleaved -ENaC compared to NSD. Mathematical modelling predicted that tubular Na+ reabsorption increased in the proximal tubule but decreased in the distal nephron because of diminished Na+ delivery. This prediction was confirmed by the natriuretic response to diuretics targeting the thick ascending limb, the distal convoluted tubule or the collecting system. On the other hand, HSD did not alter measured GFR but decreased the abundance of the aforementioned transporters compared to NSD. Mathematical modelling predicted that tubular Na+ reabsorption decreased in the proximal tubule but increased in distal segments with lower transport efficiency with respect to O2 consumption. This prediction was confirmed by the natriuretic response to diuretics. The activity of the metabolic sensor AMPK was related to the changes in tubular Na+ reabsorption. Our data show that fractional Na+ reabsorption is distributed differently according to dietary Na+ intake and induces changes in tubular O2 consumption and sodium transport efficiency. 

DOI: https://doi.org/10.1113/JP274927

# Dietary sodium induces a redistribution of the tubular metabolic workload

**Khalil Udwan[1,5], Ahmed Abed[1,5], Isabelle Roth[1], Eva Dizin[1,5], Marc Maillard[2], Carla Bettoni[3], Johannes Loffing[4,5], Carsten A. Wagner[3,5], Aurélie Edwards[4*], and Eric Feraille[1,5*]**

[1]Department of Cellular Physiology and Metabolism, University of Geneva, CMU, 1 Rue Michel-Servet, CH-1211 Geneva 4, Switzerland

[2]Centre hospitalier universitaire Vaudois, Service de néphrologie CH-1011 Lausanne, Switzerland

[3]Institute of Physiology, University of Zürich, Winterthurerstrasse 190, CH-8057 Zürich, Switzerland

[4]Institute of Anatomy, University of Zürich, Winterthurerstrasse 190, CH-8057 Zürich, Switzerland

[5]Centre de Recherche des Cordeliers, INSERM UMRS1138 and CNRS ERL8228, 15 rue de l'Ecole de Médecine, F-75006, Paris, France; Department of Biomedical Engineering, Boston University, Boston, USA

[5] National Centre of Competence in Research, NCCRKidney.CH, Switzerland

* These two authors contributed equally to this work

**Running head: Effect of dietary $Na^+$ on renal tubular transport**

Corresponding author:

Eric Feraille, Department of Cellular Physiology and Metabolism, Faculty of Medicine, University of Geneva, CMU, 1 Rue Michel Servet, 1211 Geneva 4, Switzerland

Tel: (+41) 22 379 52 82

Fax: (+41) 22 379 52 60

Email: Eric.Feraille@unige.ch

Key words: Dietary Salt, $Na^+$ transport, $Na^+$ transporters, diuretics, optimal $Na^+$ diet

## Key points

- Body $Na^+$ content is tightly controlled by regulated urinary $Na^+$ excretion.
- The intrarenal mechanisms mediating adaptation to variations in dietary $Na^+$ intake are incompletely characterized.
- We confirmed and expanded observations in mice, that variations in dietary $Na^+$ intake do not alter the glomerular filtration rate but alter the total and cell-surface expression of major $Na^+$ transporters all along the kidney tubule.
- Low dietary $Na^+$ intake increased $Na^+$ reabsorption in the proximal tubule and decreased it in more distal kidney tubule segments.
- High dietary $Na^+$ intake decreased $Na^+$ reabsorption in the proximal tubule and increased it in distal segments with lower energetic efficiency.
- We have shown that abundance of apical transporters and $Na^+$ delivery are the main determinants of $Na^+$ reabsorption along the kidney tubule.
- Tubular $O_2$ consumption and the efficiency of sodium reabsorption are dependent on sodium diet.

## Abstract

$Na^+$ excretion by the kidney varies according to dietary $Na^+$ intake. We undertook a systematic study on the effects of dietary salt intake on glomerular filtration rate (GFR) and tubular $Na^+$ reabsorption. We examined the renal adaptive response in mice subjected to 7 days of a low sodium diet (LSD) containing 0.01 % $Na^+$, a normal sodium diet (NSD) containing 0.18 % $Na^+$, as well as a moderately high sodium diet (HSD) containing 1.25 % $Na^+$. As expected, LSD did not alter measured GFR and increased the abundance of total and cell-surface NHE3, NKCC2, NCC, α-ENaC, and cleaved γ-ENaC compared to NSD. Mathematical modelling predicted that tubular $Na^+$ reabsorption increased in the proximal tubule but decreased in the distal nephron because of diminished $Na^+$ delivery. This prediction was confirmed by the natriuretic response to diuretics targeting the thick ascending limb, the distal convoluted tubule or the collecting system. On the other hand, HSD did not alter measured GFR but decreased the abundance of the aforementioned transporters compared to NSD. Mathematical modelling predicted that tubular $Na^+$ reabsorption decreased in the proximal tubule but increased in distal segments with lower transport efficiency with respect to $O_2$ consumption. This prediction was confirmed by the natriuretic response to diuretics. The activity of the metabolic sensor AMPK was related to the changes in tubular $Na^+$ reabsorption. Our data show that fractional $Na^+$ reabsorption is distributed differently according to dietary $Na^+$ intake and induces changes in tubular $O_2$ consumption and sodium transport efficiency.

## Abbreviations

AMPK, adenosine monophosphate-activated protein kinase; ATP, adenosine triphosphate; BP, blood pressure; CD, collecting duct; CKD, chronic kidney disease; CNT, connecting tubule; DCT, distal convoluted tubule; ENaC, epithelial sodium channel, HSD, high salt diet; LSD, low salt diet; NSD, normal salt diet; Na,K-ATPase, sodium, potassium, adenosine triphosphatase; PT, proximal tubule; TAL, thick ascending limb of Henle.

## Introduction

The average daily $Na^+$ intake in modern societies is largely higher than 2 g (87 mmol/24 h), the value recommended for adults by the World Health Organization 2012 guidelines (http://www.who.int/nutrition/publications/guidelines/sodium_intake/en/). A high salt intake is associated with adverse health outcomes in relation with increased blood pressure (BP) (Meneton *et al.*, 2005). Furthermore, salt may play an essential role in the progression of chronic kidney disease (CKD), which is characterized by decreased glomerular filtration rate, albuminuria as well as glomerular and tubular-interstitial fibrosis, both in BP–dependent and BP–independent manners (Boero *et al.*, 2002; Kotchen *et al.*, 2013). Conversely, dietary salt restriction has been shown to reduce BP, albuminuria, and kidney fibrosis (Lambers Heerspink *et al.*, 2012). In contrast, the few randomized controlled trials available did not clearly demonstrate the benefits of salt restriction in the general population (O'Donnell *et al.*, 2014). Moreover, recent studies suggested that both very low and high $Na^+$ intakes are associated with increased mortality, consistent with a U- or J-shaped association between urinary $Na^+$ excretion and cardiovascular outcomes (Graudal *et al.*, 2014; O'Donnell *et al.*, 2014; Pfister *et al.*, 2014). While not universally accepted (Cogswell *et al.*, 2016), this non-linear relationship between $Na^+$ intake and cardiovascular outcomes may indicate that our cardio-renal system is best adapted to an optimal range of $Na^+$ intake.

Arterial blood pressure depends on intravascular volume, which is directly proportional to plasma $Na^+$ content (Meneton *et al.*, 2005). It is traditionally accepted that under physiological conditions, plasma and interstitial compartments are in equilibrium and that any change in extracellular $Na^+$ content elicits a proportional change in extracellular water volume so as to maintain body fluid osmolality constant. In order to keep plasma volume within narrow limits, urinary $Na^+$ excretion must match as closely as possible dietary $Na^+$ intake minus skin

and digestive $Na^+$ losses. This precise adaption requires a continuous coordination between the filtered amount of $Na^+$ and its tubular reabsorption (Greger, 2000). In healthy individuals, 1-3% of the filtered $Na^+$ is not reabsorbed and is excreted in urine (Meneton *et al.*, 2005). $Na^+$ reabsorption takes place along the nephron and collecting duct, via transcellular and paracellular pathways (Féraille & Doucet, 2001). Transcellular $Na^+$ reabsorption is a two-step process: $Na^+$ enters tubular cells via a segment-specific apical transporter and is extruded by the basolateral Na,K-ATPase (Féraille & Doucet, 2001). The first step is mostly mediated by the apical $Na^+/H^+$ exchanger NHE3 in the proximal tubule (PT) (Tse *et al.*, 1992), the $Na^+/K^+/2Cl^-$ cotransporter NKCC2 in the thick ascending limb of Henle's loop (TAL) (Gamba *et al.*, 1994), and the NaCl cotransporter NCC in the distal convoluted tubule (DCT) (Gamba *et al.*, 1993). Lastly, the fine-tuning of $Na^+$ reabsorption occurs via the multimeric $Na^+$ channel ENaC under the control of aldosterone in the late DCT, connecting tubule (CNT) and collecting duct (CD) (Canessa *et al.*, 1994).

In the kidney, ATP and oxygen consumption are determined primarily by the energy required for tubular $Na^+$ reabsorption (Kiil *et al.*, 1961; Brodwall & Laake, 1964; Mandel, 1986). Transcellular $Na^+$ transport is directly dependent on the electrochemical potential generated by Na,K-ATPase, which uses 1 molecule of ATP to drive the outward transport of 3 $Na^+$ and the inward transport of 2 $K^+$. AMP-activated protein kinase (AMPK) is a key controller of cellular energy metabolism. AMPK activity which is stimulated when the AMP/ATP ratio increases reflects the intensity of active $Na^+$ handling and links it to the metabolic status of a cell (Hallows *et al.*, 2000).

The aims of the present study were to assess the respective role of changes in the abundance of the renal $Na^+$ transporters and sodium delivery in the rate of $Na^+$ transport by the different segments of the kidney tubule in response to different $Na^+$ intakes, as well as the relation between tubular $Na^+$ transport and the activity of the metabolic sensor AMPK. We

showed in normal mice that in response to a low sodium diet (LSD), the expression levels of most apical $Na^+$ transporters and Na,K-ATPase were increased while $Na^+$ transport decreased in segments downstream from the PT. Under a high sodium diet (HSD), the expression levels of most apical $Na^+$ transporters were decreased, and $Na^+$ transport decreased along the PT but increased downstream in TAL and CD in response to increased $Na^+$ delivery. The rate of $Na^+$ reabsorption by tubular segments was correlated to AMPK activity. Finally, the efficiency of tubular $Na^+$ reabsorption with respect to $O_2$ consumption was slightly higher under NSD as compared to LSD or HSD.

## Material and Methods

### Animals

Male C57B6 mice (Charles-River, Saint Germain de l'Arbresle, France) aged 12-16 weeks were fed for 7 days with either a low (0.01 % wt/wt), standard (0.18 % wt/wt) or moderately high sodium (1.25 % wt/wt) diet (Provimi-Kliba, Kaiseraugst, Switzerland). All diets contained the same amounts of potassium (0.8% wt/wt). To record physiological parameters, mice were placed in metabolic cages (Tecniplast, Buguggiate VA, Italy) under controlled conditions of light, temperature, and humidity. After 2 days of adaptation, body weight, food intake, water intake, and 24-h-period urine samples were measured and collected from day 0 to day 6 after the start of each sodium diet. Urinary creatinine, $Na^+$, $Cl^-$ and $K^+$ concentrations were determined using ion-specific electrodes (UniCel DxC800 Synchron Clinical System, Beckman Coulter). Absolute $Na^+$, $Cl^-$ and $K^+$ excretions were measured. Urinary aldosterone levels were measured according to standard procedures using the Coat-A-Count RIA kit (Siemens Medical Solutions Diagnostics, Ballerup, Denmark). After 7 days on a given sodium diet, mice were either subjected to GFR measurements, *in situ* biotinylation or sacrificed thereafter for tissue and organ removal. Animals were anaesthetized by intraperitoneal injection of ketamine and

xylazine (100 mg/kg and 5 mg/kg, respectively) (GRAEUB, Swissmedic, Bayer Healthcare). At the end of experiments, animals were deeply anaesthetized with 50 mg x kg body $wt^{-1}$ pentobarbital i.p. (Sanofi, Toulouse, France). For *in vitro* studies (microdissection and immunoblotting), animals were studied 7 days after being placed on a given $Na^+$ diet. Animal experiments were approved by the ethical committee of the University of Geneva and governmental authorities.

**Transcutaneous measurement of GFR (mGFR) in conscious mice**

For GFR measurements, mice were anesthetized with isoflurane, and a miniaturized imager device built from two light-emitting diodes, a photodiode and a battery (Mannheim Pharma and Diagnostics, Mannheim, Germany), was mounted via double-sided adhesive tape onto the shaved animal's neck. For the duration of the recording (1 h), each animal was conscious and kept in a single cage. Before the intravenous injection of 150 mg/kg FITC-sinistrin (Mannheim Pharma and Diagnostics, Germany), the skin's background signal was recorded for 5 min. After removal of the imaging device, the data were analysed using MPD Lab software (Mannheim Pharma and Diagnostics, Germany). mGFR (µL/min) was calculated from the decrease in fluorescence intensity over time (i.e., plasma half-life of FITC-sinistrin) using a two compartment model, the mouse body weight and an empirical conversion factor (Schreiber *et al.*, 2012).

**Functional diuretic tests**

On some of the animals that were fully adapted in metabolic cages, we performed diuretics response studies. Briefly, furosemide (10mg/kg), hydrochlorothiazide (50mg/kg), amiloride (5mg/kg) or benzamil (5mg/kg) were injected i.p 7 days after the onset of various $Na^+$ diets (Leviel *et al.*, 2010; Morla *et al.*, 2013; Al-Qusairi *et al.*, 2017). Urinary $Na^+$ excretion

normalized by creatinine excretion was measured 1h, 4h, or 6h, and 24 h after the injection of furosemide, hydrochlorothiazide, and amiloride or benzamil, respectively.

**Microdissection of renal tubules**

Briefly, the left kidneys of pentobarbital-anaesthetized mice were infused via the abdominal aorta with an incubation solution (Hank's solution supplemented with 1 mm pyruvate, 0.1% bovine serum albumin (BSA), 0.5 mm $MgCl_2$, 1 mm glutamine and 20 mm Hepes, pH 7.4) containing collagenase (Worthington, 337 UI mg−1, 0.18% wt/vol). Kidneys were cut into small pieces which were incubated for 20-25 min at 32°C in an oxygenated incubation solution containing 0.1% collagenase. Renal tubules, i.e. PCT, cTAL and CCD, were microdissected under stereomicroscopic observation in an incubation solution supplemented with antiproteases (Protease inhibitor cocktail tablets, Roche) at 4°C, as previously described (Gonin *et al.*, 2001). For protein analysis by Western blotting each lane represents pools of microdissected tubules from two animals.

**Immunoblotting**

Pools of 40-50 isolated tubules or 10 μg proteins extracted from kidney cortex were solubilized at 95°C for 5 min in Laemmli buffer and stored at −20°C until use. Proteins were subjected to SDS-PAGE and transferred onto polyvinylidene difluoride membranes (Immobilon-P; Millipore). After blocking in TBS–tween buffer (50 mm Tris base, 150 mm NaCl, 0.1 % tween) containing 5% non-fat dried milk, blots were successively incubated with specific antibodies. Antibodies used to detect $Na^+$ transporters are listed in Table 1. Rabbit polyclonal antibodies raised against AMPK α-subunit and ACC (Cell Signaling) were diluted 1:1000 and those raised against phospho-AMPK α-subunit and phospho-ACC (Cell Signaling) were diluted 1:500. Mouse monoclonal antibodies raised against E-Cadherin (BD Biosciences Pharmingen) were

diluted 1/1000, β-actin (Sigma) were diluted 1:20,000. Anti-βHorseradish peroxidase-conjugated secondary antibodies (BD Biosciences Pharmingen) diluted 1:20,000 (v/v) were used for detection of immunoreactive proteins by enhanced chemiluminescence (Millipore). Bands were quantified with imageJ software. Results were expressed as the ratio of the densitometry of the band of interest to the loading control.

### *In situ* mouse kidney biotinylation

Renal plasma membranes were biotinylated *in situ* as described previously (Frindt *et al.*, 2008), with some modifications. Kidneys were perfused with heparinized-TBS for washing, then they were perfused with 0.5 mg/ml sulfosuccinimidyl-2-[biotinamido]ethyl-1,3-dithiopropionate (sulfo-NHS-biotin, Campbell Science, Rockville IL) at a rate of 1ml/min for 30 minutes with a mini pump, through the descending aorta. The reaction was stopped and excess biotin was removed by further perfusion with TBS for 10 mins. At the end of the perfusion, the left kidney was quickly removed, minced with a razor blade and homogenized with a tight-fitting Dounce in 8 ml of lysis buffer containing (in mM) 250 sucrose, 10 triethanolamine HCl, 1.6 ethanolamine, 0.5 EDTA at pH 7.40 and 60 µl protease-inhibitor cocktail (Sigma-Aldrich). The homogenate was centrifuged at 1000 x g for 10 min to separate intact tissue; supernatant was collected and frozen at – 80 $^{o}$C for later use. The samples then centrifuged at 100,000 x g for 2 h to sediment a total membrane pellet. This was resuspended in 2 ml of lysis buffer, aliquoted and frozen at -80 $^{o}$C for later analysis. Protein concentrations were measured with a micro BCA reagent kit (Pierce Chemical). The isolation of biotinylated proteins used Neutravidin Ultralink beads (Pierce) as described previously for rat kidneys (Frindt & Palmer, 2015).

### Mathematical model

Model predictions of transepithelial sodium fluxes and oxygen consumption rates were obtained using a published model of transport along the superficial nephron of a rat (Layton *et*

*al.*, 2016). The model represents the tubules as cylinders, with axial flows and lateral fluxes across transcellular and paracellular pathways. It computes the transport rates of water and 12 solutes along the nephron, by considering the specific transporters (i.e., channels, exchangers, cotransporters, and pumps) that are expressed on the apical and basolateral membranes in each segment. The underlying equations express conservation of mass and charge; they are solved at steady-state to yield volume, concentrations, and electric potential in the lumen and in each cell type, as a function of position. Interstitial concentrations are assumed to be known. Active $O_2$ consumption is taken to be proportional to the Na-K-ATPase transport rate.

**Statistics** Results are given as means ± SE from *n* independent experiments. Comparisons between two groups were performed by unpaired Student's *t*-test unless stated otherwise. Comparisons between more than two groups were performed by ANOVA and Dunnet's t-test or by Kruskall-Wallis analysis of variance. A $p$ value $<0.05$ was considered significant.

## Results

**Effect of dietary $Na^+$ intake on physiological parameters**. Mice were fed for 6 days with a low sodium diet (LSD, 0.01% $Na^+$), a high sodium diet (HSD, 1.25% $Na^+$), or a normal sodium diet (NSD, 0.18% $Na^+$). All three groups displayed similar body weight and food intake (Fig. 1A-B) as well as plasma [$Na^+$] and [$K^+$] (Table 2). As expected, under NSD, urinary $Na^+$ and $Cl^-$ excretion increased slightly in parallel with the progressive increase in food intake, reflecting adaptation to metabolic cages (Fig1. E and Fig S1). Water intake and urine output increased throughout the 6 days of HSD while urinary $Na^+$ and $Cl^-$ excretion reached a steady-state after 3 days (Fig. 1C-E and Fig S1). In contrast, water intake and urinary output were unchanged while urinary $Na^+$ and $Cl^-$ excretion significantly decreased during LSD (Fig. 1C-E and Fig. S1). Urinary $K^+$ excretion displayed a progressive rise following the increase in food

intake, reflecting adaptation to metabolic cages. $K^+$ excretion was unchanged under LSD while it significantly increased under HSD (Fig. 1F). Figure 1G shows that as expected, 24 hours urinary aldosterone, measured on day 6, strongly increased after LSD and was largely decreased after HSD, as compared to NSD. This finding is in agreement with previous studies showing that changes in dietary salt intake are accompanied by inverse changes in the activity of the renin-angiotensin-aldosterone system (Masilamani *et al.*, 2002; Yang *et al.*, 2008; Castrop *et al.*, 2010). As previously reported in rats (Thomson *et al.*, 2006), GFR measured as FITC-sinistrin clearance after 7 days of diet was unchanged by LSD or HSD (Fig. 1H). These results indicate that mice achieved steady-state conditions.

**Effect of dietary $Na^+$ on apical $Na^+$ transporters and Na,K-ATPase expression**. We measured the cell surface expression of key $Na^+$ transporters in response to different $Na^+$ diets. Ion transporter activity is proportional to the number of molecules inserted into the plasma membrane and in contact with extracellular medium (Loffing *et al.*, 2001). To assess the cell-surface expression of kidney tubule $Na^+$ transporters, we adapted we adapted to mice the *in situ* biotinylation technique that had previously been applied to rats by Frindt et al (Frindt *et al.*, 2008). Results showed that LSD increased significantly the cell-surface abundance of NHE3, NKCC2, NCC, α-ENaC, as well as both cleaved and non-cleaved γ-ENaC, whereas HSD significantly decreased the apical surface abundance of all these ion transporter proteins (Fig. 2). These results suggest that LSD increased while HSD decreased overall apical $Na^+$ transporter abundance along the mouse renal tubule.

We then assessed the total abundance of kidney tubule $Na^+$ transporters by Western blotting in kidney cortex extracts. LSD compared to NSD significantly increased the total protein abundance of $Na^+/H^+$ exchanger 3 (NHE3), NKCC2, α-ENaC, and cleaved γ-ENaC (Fig. S2).

In contrast to its cell-surface abundance, the total abundance of NCC was not significantly increased but its activating phosphorylation on threonine 53 was increased (Fig. S3). HSD on the other hand significantly decreased the total expression levels of NHE3, NCC, α-ENaC, and cleaved γ-ENaC as well as phosphorylation of NCC on threonine 53 (Fig. S3). The abundance of NKCC2 and the non-cleaved form of γ-ENaC was not significantly changed under HSD (Fig. S2). These results indicate that dietary sodium-induced variations of cell-surface abundance of the major kidney tubule $Na^+$ transporters are not necessarily associated with parallel changes in their total abundance. In addition, we assessed the effect of dietary salt on H-ATPase and Pendrin, the major apical acid-base transporters of α- and β-intercalated cells, respectively. Results show that Pendrin and H-ATPase abundance were not significantly altered by changes in dietary salt intake (Fig. S3).

The ubiquitous Na,K-ATPase (dietary NKA) located along the basolateral membranes of tubular epithelial cells is the major pathway for $Na^+$ extrusion. Expression of the NKA α1-subunit, the almost exclusive kidney isoform (Féraille & Doucet, 2001), increased in both cell-surface and total kidney cortex protein extracts under LSD but remained unchanged under HSD (Figs. 2 and S2). Therefore, the abundance of NKA increases in parallel with that of apical $Na^+$ transporters under LSD, but it does not follow the general decrease in apical $Na^+$ transporters abundance observed under HSD.

**Mathematical modelling of $Na^+$ transport along the nephron**. We assessed how tubular $Na^+$ transport (TNa) was redistributed along the nephron under LSD or HSD by running simulations with a previously described mathematical model (Layton *et al.*, 2016). Since the model applies to a rat kidney, we focused on the relative changes in transepithelial transport and urinary excretion. Results were expressed as arbitrary units as opposed to their absolute values. In these

simulations, we accounted for the measured fractional changes in cell-surface expression levels (see Fig. 2), as summarized in Table 3. The predicted and measured diet-induced variations in the urinary excretion of $Na^+$ and $K^+$ were in good agreement overall (Supplementary Table 1). The computed value of overall $Na^+$ transport increased very slightly (by 1%) under LSD and decreased by 9% under HSD (Fig. 3A). The model predicts that relative to NSD, $Na^+$ reabsorption under LSD is increased in the proximal nephron (from the proximal tubule to the medullary thick ascending limb, or mTAL), and reduced in the segments downstream (Fig. 3B-X). TNa increases the most (both in absolute and relative terms) in the mTAL, given the 3.2-fold increase in the cell-surface expression of NKCC2. Downstream, TNa decreases despite the increase in transporter expression, owing to diminished $Na^+$ delivery. In particular, net $Na^+$ secretion is predicted in the CCD under LSD (Fig. 3X) because low $Na^+$ delivery to that segment strongly stimulates paracellular $Na^+$ secretion, which more than counterbalances transcellular $Na^+$ reabsorption. Thus, our results suggest that TNa is governed not only by $Na^+$ transporter abundance but also by $Na^+$ delivery to a given segment.

Conversely, the model predicts that, relative to NSD, $Na^+$ reabsorption under HSD diminishes all the way to the connecting tubule (except for the cortical thick ascending limb) and increases in the collecting duct (Fig 3. B-X). The largest TNa reduction occurs in the proximal tubule, as a result of the 2-fold reduction in NHE3 expression (Table 3). By contrast, TNa increases in the collecting duct, despite the decrease in ENaC and NKA membrane expression, because of higher $Na^+$ delivery to that segment.

**Effect of dietary $Na^+$ on $Na^+$ transporters expression in microdissected tubules**. We dissected proximal convoluted tubules (PCT), cortical thick ascending limbs of Henle (cTAL), and cortical collecting ducts (CCD) from collagenase-treated kidney cortices. In microdissected

PCTs, NHE3 expression increased under LSD while it decreased under HSD, as compared to NSD. These results are similar to those observed in cell-surface protein extracts and whole kidney cortex homogenates. On the other hand, NKA α1-subunit protein abundance increased both in LSD and HSD (Fig. 4A). In the cTAL, NKCC2 expression increased under LSD whereas α1-NKA abundance was unchanged, as compared to NSD. These results match those obtained in cell-surface protein extracts and whole kidney cortex homogenates. On the other hand, HSD altered neither NKCC2 nor α1-NKA expression levels in cTAL (Fig. 4B). This observation is in agreement with results obtained in whole kidney cortex but at variance with the observed decrease in NKCC2 abundance in cell-surface protein extracts. This result in cTAL suggests that NKCC2 abundance is largely decreased in medullary TAL under HSD. We also assessed the changes in the expression levels of ENaC subunits and NKA in the CCD, an aldosterone-sensitive tubular segment where the fine-tuning of sodium reabsorption occurs. In agreement with results obtained in cell-surface and total cortex protein extracts, LSD increased the abundance of α-ENaC and γ-ENaC subunits as well as that of α1-NKA proteins. The amount of proteins loaded on the gel was not sufficient to detect the cleaved form of γ-ENaC. On the other hand, HSD increased both α-ENaC and α1-NKA protein expression, whereas γ-ENaC abundance was unchanged (Fig. 4C). These patterns are at variance with the observed decrease in both α-ENaC and γ-ENaC in both cell-surface and total cortex protein extracts. This apparent discrepancy most likely reflects the differential control of ENaC subunit abundance in the late DCT and CNT, as compared to the CCD. We were not able to hand microdissect a large enough number of DCTs and CNTs that would allow the detection of NCC and ENaC subunits by Western blot. Taken together, our results indicate that dietary $Na^+$ intake

influences $Na^+$ transporter expression in a segment-specific pattern that is, at least partly, independent of variations in aldosterone secretion.

**Mathematical modelling of segment-specific $Na^+$ transport**. We then performed another set of simulations to account for the segment-specific, fractional changes in apical $Na^+$ transporter and NKA expression in the PCT, cTAL, and CCD. Model assumptions for this scenario (denoted case 2) are also shown in Table 3. Compared to the results obtained using only whole-kidney data (case 1, see above), the computed value of whole kidney TNa remains unchanged under LSD, and is 1% lower under HSD. The latter result may appear counter-intuitive: since Na,K-ATPase expression in the PCT, cTAL, and CCD is higher in case 2 than in case 1 under HSD, overall $Na^+$ reabsorption is expected to increase rather than to decrease. TNa is indeed higher in the cTAL and CCD (case 2 vs. case 1), but it is 4% lower in the PCT (Fig. 5), because of counterbalancing effects. [1]

Overall our results suggest that, in the absence of changes in the delivered load, the major determinant of TNa is the apical $Na^+$ transporter abundance. Given a fixed load, $Na^+$ reabsorption is predicted to decrease (relative to NSD) in segments where the expression of apical transporters decreases, even when the expression of basolateral NKA increases concomitantly. This is exemplified in the PCT where decreased $Na^+$ reabsorption under HSD is explained by decreased NHE3 expression despite increased NKA expression (Fig. 5).

**Functional assessment of nephron-segment specific $Na^+$ transporters**. Diuretics promote natriuresis and diuresis by inhibiting tubular $Na^+$ reabsorption at specific nephron sites. Loop

[1] *According to our simulations, when NHE3 expression is reduced by half, increased NaK activity in the PCT lowers the intracellular concentration of $Na^+$ such that basolateral $Na^+$ (and $HCO_3^-$) entry via $Na^+$-dependent $Cl^-/HCO_3^-$ exchangers (NDCBE) is strongly stimulated. The resulting increase in intracellular pH in turn reduces apical $Na^+/H^+$ exchange across NHE3, lowers the transepithelial voltage, and thereby reduces paracellular $Na^+$ reabsorption as well.*

diuretics inhibit NKCC2 (Velázquez & Wright, 1986) and thus $Na^+$ reabsorption in the TAL (Greger, 1985). The effect of furosemide on natriuresis measured one hour after the injection was higher under HSD and lower under LSD, as compared to NSD (Fig. 6A).

Thiazides decrease $Na^+$ reabsorption mostly by blocking NCC in the DCT (Velázquez & Wright, 1986). In response to hydrochlorothiazide, $Na^+$ excretion was higher under HSD and lower under LSD, as compared to NSD. Mice on LSD showed a higher response relative to the previous 24h $Na^+$ excretion when compared to mice on NSD and HSD (Fig. 6B). The higher absolute $Na^+$ excretion observed under HSD might be partly explained by decreased ENaC abundance in connecting tubule (see Fig. 3). This impairs the compensation of the diuretic-induced natriuresis via increased $Na^+$ reabsorption by the CNT. On the other hand, the decreased natriuretic response observed under LSD might be in part related to increased downstream ENaC-dependent $Na^+$ reabsorption by the CNT and the collecting duct (see Figs. 3 and 5).
In the aldosterone-sensitive distal nephron (ASDN, *i.e.* the distal convoluted tubule (DCT2), connecting tubule, and collecting duct), the amiloride-sensitive epithelial $Na^+$ channel ENaC, consisting of α-, β-, and γ-subunits, mediates $Na^+$ uptake across the apical plasma membrane of principal cells (Loffing & Kaissling, 2003). Figure 6C shows that the effects of amiloride on $Na^+$ excretion were higher under HSD and lower under LSD, as compared to NSD, despite the presence of higher aldosterone levels in LSD (Fig. 1H). Similar results were obtained using benzamil, a more selective inhibitor of ENaC (Barbry *et al.*, 1986) (Fig. S5). Control experiments indicate that the observed natriuresis and diuresis in response to diuretics is not affected by the intraperitoneal infusion of the vehicle (0.9 % NaCl; Fig. 6D). Increased natriuresis in response to amiloride under HSD relies at least in part on inhibition of the net $Na^+$ reabsorption that occurs along the collecting duct (see Figs. 3 and 5). In contrast, the decreased amiloride resp

onse observed under LSD may rely on increased Na delivery that inhibits $Na^+$ secretion along the collecting duct (see Figs. 3 and 5).

Using the mathematical model of transport along the nephron, we simulated the effects of furosemide, hydrochlorothiazide, and amiloride by fully and selectively inhibiting NKCC2, NCC, and ENaC, respectively. The predicted effects of these diuretics mimicked the experimental results, with increased $Na^+$ excretion under HSD and decreased $Na^+$ excretion under LSD, as compared to NSD, thereby confirming our *in vivo* results (Fig. 6E).

**Regulation of AMPK activity by dietary $Na^+$ intake**. Increasing transcellular $Na^+$ reabsorption by renal epithelial cells augments ATP consumption and thus results in an increased cytosolic AMP-to-ATP ratio that may activate AMP-activated protein kinase (AMPK), as previously suggested in γ-ENaC-TetOn-mCCD cells (Wang *et al.*, 2014). We estimated the activity of AMPK in total kidney extracts from mice subjected to various salt diets. Under HSD the phosphorylation levels of AMPK α-subunit and its substrate acetyl-CoA carboxylase (ACC) were significantly increased, reflecting an increase in AMPK activity (Fig 7). To further assess the changes in AMPK activity along the kidney tubule, we microdissected specific nephron segments (PCT, cTAL, and CCD) and measured the amounts of total and phosphorylated ACC. We found that under HSD, pACC was significantly increased in cTALs and CCDs (Fig. 8A-C). LSD, on the other hand, increased pACC in PCTs (Fig. 8A) whereas it remained unchanged in cTALs and CCDs (Fig. 8B-C). These changes in AMPK activity were positively correlated with estimated increases in active $Na^+$ reabsorption in PCTs and CCDs, and cTALs (see Fig. 5).

**Modelling of segment-specific $O_2$ consumption and tubular $Na^+$ transport efficiency**. Tubular $Na^+$ reabsorption is an active process that consumes both ATP and $O_2$. Simulations of

$Na^+$ transport in specific nephron segments indicate that $O_2$ consumption rose in cTALs under HSD and in PCTs and CCDs under LSD (Fig. 9A). Our model also suggests that the overall efficiency of $Na^+$ transport, as reflected by the whole nephron ratio of TNa to active $O_2$ consumption (denoted $TNa/QO_2$), decreased slightly under both diets. As shown in Figure 9B, $TNa/QO_2$ was highest in the PT, where paracellular and transcellular transport contribute almost equally to $Na^+$ reabsorption; $TNa/QO_2$ was significantly lower in downstream segments, where $Na^+$ backleak across the paracellular pathway can partially counteract transcellular $Na^+$ reabsorption. In HSD, a significant fraction of $Na^+$ transport was shifted from the PCT to downstream segments, hence the predicted decrease in transport efficiency. In LSD, the increase in NHE3 abundance enhanced the contribution of the transcellular pathway relative to that of the paracellular pathway in the PT, which is why $TNa/QO_2$ was predicted to decrease in this case as well. Overall, these results suggest that changes in dietary salt intake elicit a redistribution of $O_2$ consumption along the kidney tubule.

## Discussion

The objective of this study was to revisit the patterns of the kidneys' adaptive response to dietary $Na^+$ changes using a combination of measurements of physiological parameters and $Na^+$ transporter protein abundance, functional response to diuretic tests, and mathematical modelling. Indeed, previous studies analysed separately the effect of dietary $Na^+$ on either GFR or $Na^+$ transporters abundance but to our knowledge, none of them performed a complete analysis of the effects of dietary $Na^+$ content. Our results show that plasma $Na^+$ levels and GFR did not change after one week on a diet containing various amounts of $Na^+$. This means that the filtered $Na^+$ load remained similar under all conditions studied. In addition, previous studies have shown that systemic blood pressure (BP) does not change under these short periods of

altered diet (Holtbäck *et al.*, 1993; Meneton *et al.*, 2005; Brochu *et al.*, 2013; Walkowska *et al.*, 2016). Therefore, alterations in natriuresis were only due to changes in $Na^+$ handling along the renal tubule.

Our results show that under LSD, the mouse kidney reduces urinary $Na^+$ excretion, which is associated with increased expression of NHE3 in PTs, NKCC2 in TALs, NCC in DCTs, and ENaC subunits in CNTs/CDs. A previous study using the same methodology indicated that in rats, LSD for 1 week did not alter both total and cell-surface abundance of NHE3 and NKCC2, revealing species differences. In contrast, cell-surface NCC and both total and cell surface abundance of ENaC subunits were increased in both mice (our study) and rats (Frindt & Palmer, 2009). As previously shown in rats (Frindt & Palmer, 2009), the increase in ENaC subunit abundance observed in our mouse study is most likely dependent on increased aldosterone levels. Our simulations of tubular $Na^+$ transport showed that $Na^+$ reabsorption was increased in the PT as also reflected by a rise in AMPK activity, leading to decreased downstream $Na^+$ delivery and $Na^+$ reabsorption. This interpretation is confirmed by the reduced natriuretic response to diuretics targeting the TAL, DCT, and CNT/CD.

The present study demonstrates that the mouse kidney adapts to a moderate HSD by increasing urinary $Na^+$ and $Cl^-$ excretion, which is associated with decreased cell-surface abundance of NHE3 in PTs, NKCC2 in TALs, NCC in DCTs, and ENaC subunits in CNTs/CDs. At variance with our findings in mice, Frindt and Palmer found that total and cell-surface NHE3, NKCC2 and NCC abundance were not altered in rats fed with a HSD (5 % NaCl) for 1 week. These differences may rely on different protocols (5% vs 3% NaCl) and species specific effects. However, α- and γ-ENaC total and cell-surface abundance were similarly decreased in both mice and rats (Frindt & Palmer, 2009). Our simulations of tubular $Na^+$ transport indicated that decreased $Na^+$ reabsorption by the kidney mostly results from decreased $Na^+$ reabsorption by the PT. This adaptation of $Na^+$ transport in the PT increased $Na^+$ delivery and may lead to

increased metabolic work downstream. On the whole, the calculated efficiency of whole-nephron tubular $Na^+$ transport was only slightly decreased. Alteration of the efficiency of tubular $Na^+$ transport has been also reported under conditions that alter NO synthesis, such as treatment with a NO synthase blocker or 5/6 nephrectomy (Epstein *et al.*, 1994; Welch *et al.*, 2005). It should be mentioned that more subtle changes occur at the level of specific nephron segments such as the CCD, where increased expression of α-ENaC and Na,K-ATPase α1-subunit are observed. These alterations cannot be due to increased aldosterone levels and imply that regulation of $Na^+$ transport by the collecting duct occurs via both aldosterone-dependent and -independent mechanisms that may rely on secretion of paracrine factors such as the recently described α-ketoglutarate pathway (Grimm *et al.*, 2015).

Whether NHE3 is regulated by dietary $Na^+$ remained controversial. In one study, NHE3 expression was found to increase after salt restriction (Fisher *et al.*, 2001). Other studies showed no change in NHE3 abundance in response to alterations in dietary $Na^+$ (Masilamani et al., 2002; Thomson et al., 2006; Yang et al., 2008), or else found that HSD induces a redistribution of NHE3 from the top to the base of the microvilli (Yang *et al.*, 2008). Our results indicate that under steady-state conditions, HSD decreases both NHE3 expression and $Na^+$ transport along the mouse PT while LSD results in opposite changes. In accordance with our results, Thomson et al (Thomson *et al.*, 2006) reported that in rats, salt loading for 7 days decreased $Na^+$ transport in the PT.

Some studies showed no changes in the abundance of NKCC2 with HSD (Ecelbarger *et al.*, 1996; Yang *et al.*, 2008), while others found increased NKCC2 abundance in response to chronic saline loading (Song *et al.*, 2004). Loffing et al.(Loffing *et al.*, 2000) previously found that in rat HSD decreased α-ENaC expression and induced a redistribution of β-ENaC and γ-ENaC from apical to intracellular pools. We found that HSD decreased the whole-kidney

expression of all ENaC subunits, whereas in microdissected CCDs the expression of α-ENaC increased but not that of γ-ENaC. This observation implies that ENaC expression diminishes in the late DCT and connecting tubule (CNT) but not in the CCD, an interpretation that is strongly supported by mathematical model simulations (see Fig. 3).

Tubular $Na^+$ reabsorption is the major source of ATP and oxygen consumption in the kidney (LASSEN & THAYSEN, 1961; BRODWALL & LAAKE, 1964; Mandel, 1986), and AMPK activity may reflect the intensity of active $Na^+$ handling (Hallows *et al.*, 2000). We have previously shown that enhanced $Na^+$ transport in cultured CD principal cells (Wang *et al.*, 2014) increased AMPK α-subunit and ACC phosphorylation (Ha *et al.*, 1994), indicating AMPK activation. Hallows et al. (Hallows *et al.*, 2000) suggested that AMPK may link cellular metabolism and ion transport. In the present study, we found a globally positive relationship between estimated $Na^+$ transport and AMPK activity in isolated nephron segments. Therefore, AMPK activity as estimated by phosphorylated ACC may represent an indication of increased tubular $Na^+$ transport.

In conclusion, our results show that in response to variations in dietary salt intake, changes in tubular $Na^+$ transport occur via both regulations of transporter expression as well as $Na^+$ delivery. This study suggests that $Na^+$ transport along a given segment is strongly impacted by $Na^+$ delivery to that segment. In addition, our results indicate that variations in dietary $Na^+$ induces a redistribution tubular $Na^+$ transport in the mouse kidney. These findings should be further confirmed in humans.

**Acknowledgements:** This work was supported by the National Center of Competence in Research Kidney control of homeostasis and a Swiss National Science Foundation grant 31003A_156736/1 to EF and 31003A_155959 to CAW. We thank Dr. Lawrence Palmer (Professor of Physiology and Biophysics, Cornell University, USA) for the protocol for *in vivo* biotinylation in mice. KU received funding within the frame of IKPP2 from the European Union's Seventh Framework Programme for research, technological development and demonstration under grant agreement no 608847.

**Author contributions**

K U: designed research studies, conducted experiments, acquired data, analysed data, and wrote manuscript

A A: designed research studies, conducted experiments, acquired data

I R: conducted experiments, acquired data, analysed data

E D: conducted experiments, acquired data

M M: performed aldosterone level measurements

C B: performed GFR measurements and metabolic cage experiments

CAW: designed in vivo research studies

JL: provided material, designed experiments, analysed data

A E: designed research studies, performed mathematical model simulations, analysed data, and wrote manuscript

E F: designed research studies, conducted experiments, analysed data, and wrote manuscript

## All authors read and approved the manuscript.

# References


Al-Qusairi L, Basquin D, Roy A, Rajaram RD, Maillard MP, Subramanya AR & Staub O. (2017). Renal Tubular Ubiquitin-Protein Ligase NEDD4-2 Is Required for Renal Adaptation during Long-Term Potassium Depletion. *J Am Soc Nephrol*.

Barbry P, Frelin C, Vigne P, Cragoe EJ & Lazdunski M. (1986). [3H]phenamil, a radiolabelled diuretic for the analysis of the amiloride-sensitive $Na^+$ channels in kidney membranes. *Biochem Biophys Res Commun* **135,** 25-32.

Boero R, Pignataro A & Quarello F. (2002). Salt intake and kidney disease. *J Nephrol* **15,** 225-229.

Brochu I, Houde M, Desbiens L, Simard E, Gobeil F, Semaan W, Bkaily G & D'Orléans-Juste P. (2013). High salt-induced hypertension in B2 knockout mice is corrected by the ETA antagonist, A127722. *Br J Pharmacol* **170,** 266-277.

Brodwall EK & Laake H. (1964). The relation between oxygen consumption and transport of sodium in the human kidney. *Scand J Clin Lab Invest* **16,** 281-286.

Canessa CM, Schild L, Buell G, Thorens B, Gautschi I, Horisberger JD & Rossier BC. (1994). Amiloride-sensitive epithelial $Na^+$ channel is made of three homologous subunits. *Nature* **367,** 463-467.

Castrop H, Höcherl K, Kurtz A, Schweda F, Todorov V & Wagner C. (2010). Physiology of kidney renin. *Physiol Rev* **90,** 607-673.

Cogswell ME, Mugavero K, Bowman BA & Frieden TR. (2016). Dietary Sodium and Cardiovascular Disease Risk--Measurement Matters. *N Engl J Med* **375,** 580-586.

Ecelbarger CA, Terris J, Hoyer JR, Nielsen S, Wade JB & Knepper MA. (1996). Localization and regulation of the rat renal $Na^+$-$K^+$-$2Cl^-$ cotransporter, BSC-1. *Am J Physiol* **271,** F619-628.

Epstein FH, Agmon Y & Brezis M. (1994). Physiology of renal hypoxia. *Ann N Y Acad Sci* **718,** 72-81; discussion 81-72.

Féraille E & Doucet A. (2001). Sodium-potassium-adenosinetriphosphatase-dependent sodium transport in the kidney: hormonal control. *Physiol Rev* **81,** 345-418.

Fisher KA, Lee SH, Walker J, Dileto-Fang C, Ginsberg L & Stapleton SR. (2001). Regulation of proximal tubule sodium/hydrogen antiporter with chronic volume contraction. *Am J Physiol Renal Physiol* **280,** F922-926.

Frindt G, Ergonul Z & Palmer LG. (2008). Surface expression of epithelial Na channel protein in rat kidney. *J Gen Physiol* **131,** 617-627.

Frindt G & Palmer LG. (2009). Surface expression of sodium channels and transporters in rat kidney: effects of dietary sodium. *Am J Physiol Renal Physiol* **297,** F1249-1255.

Frindt G & Palmer LG. (2015). Acute effects of aldosterone on the epithelial Na channel in rat kidney. *Am J Physiol Renal Physiol* **308,** F572-578.

Gamba G, Miyanoshita A, Lombardi M, Lytton J, Lee WS, Hediger MA & Hebert SC. (1994). Molecular cloning, primary structure, and characterization of two members of the mammalian electroneutral sodium-(potassium)-chloride cotransporter family expressed in kidney. *J Biol Chem* **269,** 17713-17722.

Gamba G, Saltzberg SN, Lombardi M, Miyanoshita A, Lytton J, Hediger MA, Brenner BM & Hebert SC. (1993). Primary structure and functional expression of a cDNA encoding the thiazide-sensitive, electroneutral sodium-chloride cotransporter. *Proc Natl Acad Sci U S A* **90,** 2749-2753.

Gonin S, Deschênes G, Roger F, Bens M, Martin PY, Carpentier JL, Vandewalle A, Doucet A & Féraille E. (2001). Cyclic AMP increases cell surface expression of functional Na,K-ATPase units in mammalian cortical collecting duct principal cells. *Mol Biol Cell* **12,** 255-264.

Graudal N, Jürgens G, Baslund B & Alderman MH. (2014). Compared with usual sodium intake, low- and excessive-sodium diets are associated with increased mortality: a meta-analysis. *Am J Hypertens* **27,** 1129-1137.

Greger R. (1985). Ion transport mechanisms in thick ascending limb of Henle's loop of mammalian nephron. *Physiol Rev* **65,** 760-797.

Greger R. (2000). Physiology of renal sodium transport. *Am J Med Sci* **319,** 51-62.

Grimm PR, Lazo-Fernandez Y, Delpire E, Wall SM, Dorsey SG, Weinman EJ, Coleman R, Wade JB & Welling PA. (2015). Integrated compensatory network is activated in the absence of NCC phosphorylation. *J Clin Invest* **125,** 2136-2150.

Ha J, Daniel S, Broyles SS & Kim KH. (1994). Critical phosphorylation sites for acetyl-CoA carboxylase activity. *J Biol Chem* **269,** 22162-22168.

Hallows KR, Raghuram V, Kemp BE, Witters LA & Foskett JK. (2000). Inhibition of cystic fibrosis transmembrane conductance regulator by novel interaction with the metabolic sensor AMP-activated protein kinase. *J Clin Invest* **105,** 1711-1721.

Holtbäck U, Aperia A & Celsi G. (1993). High salt alone does not influence the kinetics of the Na(+)-H+ antiporter. *Acta Physiol Scand* **148,** 55-61.

Kiil F, Aukland K & Refsum HE. (1961). Renal sodium transport and oxygen consumption. *Am J Physiol* **201,** 511-516.

Kotchen TA, Cowley AW & Frohlich ED. (2013). Salt in health and disease--a delicate balance. *N Engl J Med* **368,** 2531-2532.

Lambers Heerspink HJ, Navis G & Ritz E. (2012). Salt intake in kidney disease--a missed therapeutic opportunity? *Nephrol Dial Transplant* **27,** 3435-3442.

Lassen UV & Thaysen JH. (1961). Correlation between sodium transport and oxygen consumption in isolated renal tissue. *Biochim Biophys Acta* **47,** 616-618.

Layton AT, Vallon V & Edwards A. (2016). Predicted consequences of diabetes and SGLT inhibition on transport and oxygen consumption along a rat nephron. *Am J Physiol Renal Physiol* **310,** F1269-1283.

Leviel F, Hübner CA, Houillier P, Morla L, El Moghrabi S, Brideau G, Hassan H, Hatim H, Parker MD, Kurth I, Kougioumtzes A, Sinning A, Pech V, Riemondy KA, Miller RL, Hummler E, Shull GE, Aronson PS, Doucet A, Wall SM, Chambrey R & Eladari D. (2010). The $Na^+$-dependent chloride-bicarbonate exchanger SLC4A8 mediates an electroneutral $Na^+$ reabsorption process in the renal cortical collecting ducts of mice. *J Clin Invest* **120,** 1627-1635.

Loffing J & Kaissling B. (2003). Sodium and calcium transport pathways along the mammalian distal nephron: from rabbit to human. *Am J Physiol Renal Physiol* **284,** F628-643.

Loffing J, Pietri L, Aregger F, Bloch-Faure M, Ziegler U, Meneton P, Rossier BC & Kaissling B. (2000). Differential subcellular localization of ENaC subunits in mouse kidney in response to high- and low-Na diets. *Am J Physiol Renal Physiol* **279,** F252-258.

Loffing J, Zecevic M, Féraille E, Kaissling B, Asher C, Rossier BC, Firestone GL, Pearce D & Verrey F. (2001). Aldosterone induces rapid apical translocation of ENaC in early portion of renal collecting system: possible role of SGK. *Am J Physiol Renal Physiol* **280,** F675-682.

Lourdel S, Loffing J, Favre G, Paulais M, Nissant A, Fakitsas P, Créminon C, Féraille E, Verrey F, Teulon J, Doucet A & Deschênes G. (2005). Hyperaldosteronemia and activation of the epithelial sodium channel are not required for sodium retention in puromycin-induced nephrosis. *J Am Soc Nephrol* **16,** 3642-3650.

Mandel LJ. (1986). Primary active sodium transport, oxygen consumption, and ATP: coupling and regulation. *Kidney Int* **29,** 3-9.

Masilamani S, Wang X, Kim GH, Brooks H, Nielsen J, Nielsen S, Nakamura K, Stokes JB & Knepper MA. (2002). Time course of renal Na-K-ATPase, NHE3, NKCC2, NCC, and ENaC abundance changes with dietary NaCl restriction. *Am J Physiol Renal Physiol* **283,** F648-657.

Meneton P, Jeunemaitre X, de Wardener HE & MacGregor GA. (2005). Links between dietary salt intake, renal salt handling, blood pressure, and cardiovascular diseases. *Physiol Rev* **85,** 679-715.

Morla L, Brideau G, Fila M, Crambert G, Cheval L, Houillier P, Ramakrishnan S, Imbert-Teboul M & Doucet A. (2013). Renal proteinase-activated receptor 2, a new actor in the control of blood pressure and plasma potassium level. *J Biol Chem* **288,** 10124-10131.

O'Donnell M, Mente A, Rangarajan S, McQueen MJ, Wang X, Liu L, Yan H, Lee SF, Mony P, Devanath A, Rosengren A, Lopez-Jaramillo P, Diaz R, Avezum A, Lanas F, Yusoff K, Iqbal R, Ilow R, Mohammadifard N, Gulec S, Yusufali AH, Kruger L, Yusuf R, Chifamba J, Kabali C, Dagenais G, Lear SA, Teo K, Yusuf S & Investigators P. (2014). Urinary sodium and potassium excretion, mortality, and cardiovascular events. *N Engl J Med* **371,** 612-623.

Pfister R, Michels G, Sharp SJ, Luben R, Wareham NJ & Khaw KT. (2014). Estimated urinary sodium excretion and risk of heart failure in men and women in the EPIC-Norfolk study. *Eur J Heart Fail* **16,** 394-402.

Pruijm M, Hofmann L, Maillard M, Tremblay S, Glatz N, Wuerzner G, Burnier M & Vogt B. (2010). Effect of sodium loading/depletion on renal oxygenation in young normotensive and hypertensive men. *Hypertension* **55,** 1116-1122.

Schreiber A, Shulhevich Y, Geraci S, Hesser J, Stsepankou D, Neudecker S, Koenig S, Heinrich R, Hoecklin F, Pill J, Friedemann J, Schweda F, Gretz N & Schock-Kusch D. (2012). Transcutaneous measurement of renal function in conscious mice. *Am J Physiol Renal Physiol* **303,** F783-788.

Song J, Hu X, Shi M, Knepper MA & Ecelbarger CA. (2004). Effects of dietary fat, NaCl, and fructose on renal sodium and water transporter abundances and systemic blood pressure. *Am J Physiol Renal Physiol* **287,** F1204-1212.

Sorensen MV, Grossmann S, Roesinger M, Gresko N, Todkar AP, Barmettler G, Ziegler U, Odermatt A, Loffing-Cueni D & Loffing J. (2013). Rapid dephosphorylation of the renal sodium chloride cotransporter in response to oral potassium intake in mice. *Kidney Int* **83,** 811-824.

Thomson SC, Deng A, Wead L, Richter K, Blantz RC & Vallon V. (2006). An unexpected role for angiotensin II in the link between dietary salt and proximal reabsorption. *J Clin Invest* **116,** 1110-1116.

Titze J. (2014). Sodium balance is not just a renal affair. *Curr Opin Nephrol Hypertens* **23,** 101-105.

Tse CM, Brant SR, Walker MS, Pouyssegur J & Donowitz M. (1992). Cloning and sequencing of a rabbit cDNA encoding an intestinal and kidney-specific $Na^+/H^+$ exchanger isoform (NHE-3). *J Biol Chem* **267,** 9340-9346.

Velázquez H & Wright FS. (1986). Effects of diuretic drugs on Na, Cl, and K transport by rat renal distal tubule. *Am J Physiol* **250,** F1013-1023.

Wagner CA, Loffing-Cueni D, Yan Q, Schulz N, Fakitsas P, Carrel M, Wang T, Verrey F, Geibel JP, Giebisch G, Hebert SC & Loffing J. (2008). Mouse model of type II Bartter's syndrome. II. Altered expression of renal sodium- and water-transporting proteins. *Am J Physiol Renal Physiol* **294,** F1373-1380.

Walkowska A, Pawlak M, Jane SM, Kompanowska-Jezierska E & Wilanowski T. (2016). Effects of high and low sodium diet on blood pressure and heart rate in mice lacking the functional Grainyhead-like 1 gene. *Physiol Res*.

Wang YB, Leroy V, Maunsbach AB, Doucet A, Hasler U, Dizin E, Ernandez T, de Seigneux S, Martin PY & Féraille E. (2014). Sodium transport is modulated by p38 kinase-dependent cross-talk between ENaC and Na,K-ATPase in collecting duct principal cells. *J Am Soc Nephrol* **25,** 250-259.

Welch WJ, Blau J, Xie H, Chabrashvili T & Wilcox CS. (2005). Angiotensin-induced defects in renal oxygenation: role of oxidative stress. *Am J Physiol Heart Circ Physiol* **288,** H22-28.

Yang LE, Sandberg MB, Can AD, Pihakaski-Maunsbach K & McDonough AA. (2008). Effects of dietary salt on renal $Na^+$ transporter subcellular distribution, abundance, and phosphorylation status. *Am J Physiol Renal Physiol* **295,** F1003-1016.

## Figure Legends

**Figure 1.** Effect of dietary $Na^+$ intake on physiological parameters in mice. Body weight slightly decreased over the experimental period for all mice but without any detectable difference between LSD, NSD and HSD groups (A). Food intake was similar in all groups under various dietary salt intakes (B). Compared to LSD and NSD, HSD mice displayed a significant increase in water intake (C) and urinary volume (D). Urinary $Na^+$ excretion was highly increased under HSD and decreased under LSD as compared to NSD (E). Urinary $K^+$ excretion displayed a progressive rise following the increase in food intake reflecting the adaptation of animals to the metabolic cage. $K^+$ excretion was unchanged under LSD while it significantly increased under HSD (F). Urinary aldosterone measured at day 7 revealed a 2.5-fold increase in the LSD group and about a 2.5-fold decrease in the HSD group, as compared to the NSD group (G). After 7 days, mGFR was similar in mice under various salt diets (H). Values are means ± SEM from 6-8 mice in each group. LSD and HSD were compared to NSD; *P < 0.05, **P < 0.01, ***P < 0.001.

**Figure 2.** Cell-surface expression of $Na^+$ transporters and channel subunits under different $Na^+$ diets. After 7 days on different salt diets, cell-surface proteins were biotinylated in vivo and biotinylated proteins were extracted by precipitation of streptavidin-agarose beads and separated by SDS-PAGE. (A) Representative Western blotting experiments for the main $Na^+$ transporters, namely NHE3, NKCC2, NCC, α-ENaC, γ-ENaC, and α1−NKA. (B) Bar graphs show densitometric quantification of Western blots. The plasma membrane protein E-Cadherin was taken as a loading control. Statistical analysis showed a significant decrease in the cell-surface expression of apical NHE3, NKCC2, NCC, α-ENaC, and the cleaved and non-cleaved

forms of γ-ENaC in HSD mice. All these transporters in addition to α1–NKA were over-expressed in LSD animals. Values are means ± SEM from 4 mice in each group. LSD and HSD were compared to NSD; *P < 0.05, **P < 0.01, ***P < 0.001.

**Figure 3.** Mathematical modelling of tubular $Na^+$ transport under different salt diets. Using an *in silico* model of $Na^+$ transport along the renal tubules, we computed the rates of $Na^+$ transport (TNa) along the nephron. Results account for the fractional changes in cell-surface expression as listed in Table X (case 1). They are given in arbitrary units, since the model strictly applies to a rat kidney. Shown is the predicted TNa for the whole nephron (A), and for specific tubular segments, namely the PCT (B), cTAL (C), and CCD (D). Relative to NSD, $Na^+$ reabsorption under LSD is predicted to increase in PCTs and to decrease in cTALs and CCDs. Conversely, $Na^+$ reabsorption under HSD is predicted to decrease in PCTs and to increase in cTALs and CCDs.

**Figure 4. The effect of different salt diets on the expression of $Na^+$ transporters in microdissected tubules**: After 7 days on different salt diets, isolated well-defined nephron segments were microdissected from collagenase-treated kidneys. Pools of 100 tubules from 2 different animals were lysed and proteins were separated by SDS-PAGE followed by Western blotting and densitometric quantification. (A) Abundance of NHE3 and α1–NKA increased in PCTs from mice under LSD. In PCTs from mice under HSD, NHE3 expression decreased while α1–NKA abundance increased. (B) NKCC2 expression significantly increased and slightly decreased in TALs from mice under LSD or HSD, respectively. α1–NKA expression was unchanged. (C) In CCDs, α-ENaC and NKA expression were significantly increased in mice under both LSD and HSD. However, γ-ENaC abundance was increased only in mice under

LSD. Each lane represents protein level from tubules pooled from two independent animals. Values are means ± SEM from 3 pools from 6 mice in each group (microdissected tubules from 2 animals are pooled in the same lane). LSD and HSD were compared to NSD; *P < 0.05, **P < 0.01, ***P < 0.001.

**Figure 5. Mathematical modelling of $Na^+$ transport in isolated nephron segments under different salt diets.** TNa was determined accounting for the specific changes in transporter expression in the PCT, cTAL, and CCD (Table X, case 2). Results are given for the whole nephron (A), the PCT (B), cTAL (C), and CCD (D). Model predictions under LSD are very similar to those shown in Figure 3. Relative to NSD, NaK expression under HSD was higher in the PCT, cTAL, and CCD; whole-kidney TNa was nevertheless lower, because the decrease in apical $Na^+$ transporter expression was the dominant factor.

**Figure 6.** Functional assessment of renal sodium reabsorption in response to diuretics. After 7 days on different salt diets, mice were injected i.p. with a single dose of (A) furosemide, which inhibits NKCC2 in the TAL, (B) hydrocholorothiazide, which inhibits NCC in the DCT, (C) amiloride, which inhibits ENaC in the CNT-CD, or (D) the same volume of 0.9% NaCl. The left panels show steady-state $Na^+$ excretion 24h before diuretic administration, the middle panels show the natriuretic response to diuretics (1h for furosemide, 6h for hydrochlorothiazide, and 4h for amiloride), and the right panels show $Na^+$ excretion during the 24h recovery period. In response to each diuretic tested, the natriuretic response was the largest in mice under HSD, intermediate in mice under NSD, and the lowest in mice under LSD. (E). Simulation of the effect of furosemide, hydrochlorothiazide and amiloride on $Na^+$ excretion using a mathematical model of tubular $Na^+$ transport. Values are means ± SEM from 6 mice in each group. LSD and HSD were compared to NSD; **P < 0.01, ***P < 0.001.

**Figure 7.** Regulation of AMPK expression and activity by dietary salt in total kidney lysates. After 7 days on different salt diets, kidneys were harvested and total proteins were extracted and separated by SDS-PAGE. (A) Western blotting experiments for the 5' AMP-activated protein kinase (AMPK) pathway including total and phosphorylated AMPK (pAMPK) in addition to total (ACC) and phosphorylated Acetyl-CoA carboxylase (pACC). Representative immunoblots from 3 animals from each group are shown. (B) Bar graphs show densitometric quantification of Western blots. β-Actin was used as a loading control. Statistical analysis showed a significant increase in pAMPK and pACC levels in kidneys from mice under HSD. LSD induced a significant reduction in total AMPK abundance but increased the phosphorylation level of ACC (b). Values are means ± SEM from 6 mice in each group. LSD and HSD were compared to NSD; *p < 0.05, **p < 0.01, ***p < 0.001.

**Figure 8.** Regulation of AMPK activity by dietary salt in microdissected tubules. After 7 days on different salt diets, isolated well-defined nephron segments were microdissected from collagenase-treated kidneys. Pools of 100 tubules from 2 different animals were lysed and proteins were separated by SDS-PAGE followed by Western blotting and densitometric quantification. A representative Western blotting for total (ACC) and phosphorylated ACC (pACC) is shown in upper panels. Bar graphs show densitometric quantification of Western blots are shown in lower panels. β-Actin was used as a loading control. (A) Both HSD and LSD increased the abundance of pACC without changing the total form of this protein in PCTs. (B) In cTALs, only HSD increased pACC levels (b). In CCDs, pACC levels were significantly increased in response to HSD (C). Each lane represents protein level from tubules pooled from two independent animals. Values are means ± SEM from 3 pools from 6 mice in each group (microdissected tubules from 2 animals are pooled in the same lane). LSD and HSD were compared to NSD; *P < 0.05, **P < 0.01, ***P < 0.001.

**Figure 9. Mathematical modelling of oxygen consumption and the efficiency of $Na^+$ transport in isolated nephron segments under different salt diets.** The rate of $O_2$ consumption ($QO_2$; A) and the efficiency of $Na^+$ transport (TNa/QO2; B) were computed using an *in silico* model of $Na^+$ transport along the nephron. In HSD, $QO_2$ decreased in PCTs and CCDs but increased in cTALs (A); nevertheless, $Na^+$ transport efficiency decreased in PCTs and increased in both cTALs and CCDs, owing to the redistribution of paracellular and transcellular transport (B). In LSD**,** $QO_2$ increased in PCTs and CCDs and decreased in cTALs (A); $Na^+$ transport efficiency decreased in PCTs and cTALs (B). Whole-kidney efficiency was decreased in both the LSD and HSD groups, as compared to the NSD group.

## Tables

**Table 1: Antibodies used for Western blots**

| Name | Specie | dilution | Supplier | Reference |
|---|---|---|---|---|
| NHE3 | Mouse | 1/500 | Millipore | [NHI59] |
| NKCC2 | Rabbit | 1/1000 | J Loffing | Wagner *et al.*, 2008 |
| NCC | Rabbit | 1/1000 | J Loffing | Sorensen *et al.*, 2013 |
| NCC-pT53 | Rabbit | 1/1000 | J Loffing | Sorensen *et al.*, 2013 |
| α-ENaC | Rabbit | 1/1000 | J Loffing | Wagner *et al.*, 2008 |
| γ-ENaC | Rabbit | 1/1000 | Stressmark | [NAC205] |
| α–Na,KATPase | Rabbit | 1/1000 | E Feraille | Lourdel *et al.*, 2005 |

**Table 2: Plasma parameters**

| Diet | $Na^+$ (mM) | $K^+$ (mM) | Creatinine (mg/dl) |
|---|---|---|---|
| LSD | 155.3 ± 1.5 (7) | 4.45 ± 0.13 (7) | 0.15 ± 0.006 (7) |
| NSD | 155 ± 0.4 (6) | 4.5 ± 0.21 (6) | 0.18 ± 0.013 (6) |
| HSD | 154.4± 0.6 (8) | 4.3± 0.12 (8) | 0.17± 0.010 (8) |

**Table 3. Fractional changes in transporter expression assumed in model simulations**

| Transporter expression relative to NSD | LSD | HSD |
|---|---|---|
| NHE3 in PT | +54% | -48% |
| Na,K-ATPase in PT | +85% (+104%) | -9% (+55%) |
| NKCC2 in mTAL | +219% | -51% |
| Na,K-ATPase in mTAL | +85% | -9% |
| NKCC2 in cTAL | +219% (+32%) | -51% (-18%) |
| Na,K-ATPase in cTAL | +85% (+9%) | -9% (+4%) |
| NCC in DCT | +42% | -52% |
| Na,K-ATPase in DCT | +85% | -9% |
| ENaC in CCD | +118% | -85% |
| Na,K-ATPase in CCD | +85% (+92%) | -9% (+279%) |
| ENaC in CNT, OMCD, IMCD | +118% | -85% |
| Na,K-ATPase in CNT, OMCD, IMCD | +85% | -9% |
| Pendrin in CNT and CCD | +25% | -2% |
| Apical H-ATPase in CNT, CCD, OMCD | - | -15% |

PT, proximal tubule; mTAL/cTAL, medullary/cortical thick ascending limb of Henle; DCT, distal convoluted tubule; CNT: connecting tubule; CCD, cortical collecting duct; OMCD/IMCD, outer/inner medullary collecting duct. Fractional changes were measured using an *in situ* biotinylation technique or total protein extracts (Pendrin and H-ATPase). Values in parentheses correspond to segment-specific results (case 2), as opposed to whole-kidney values.

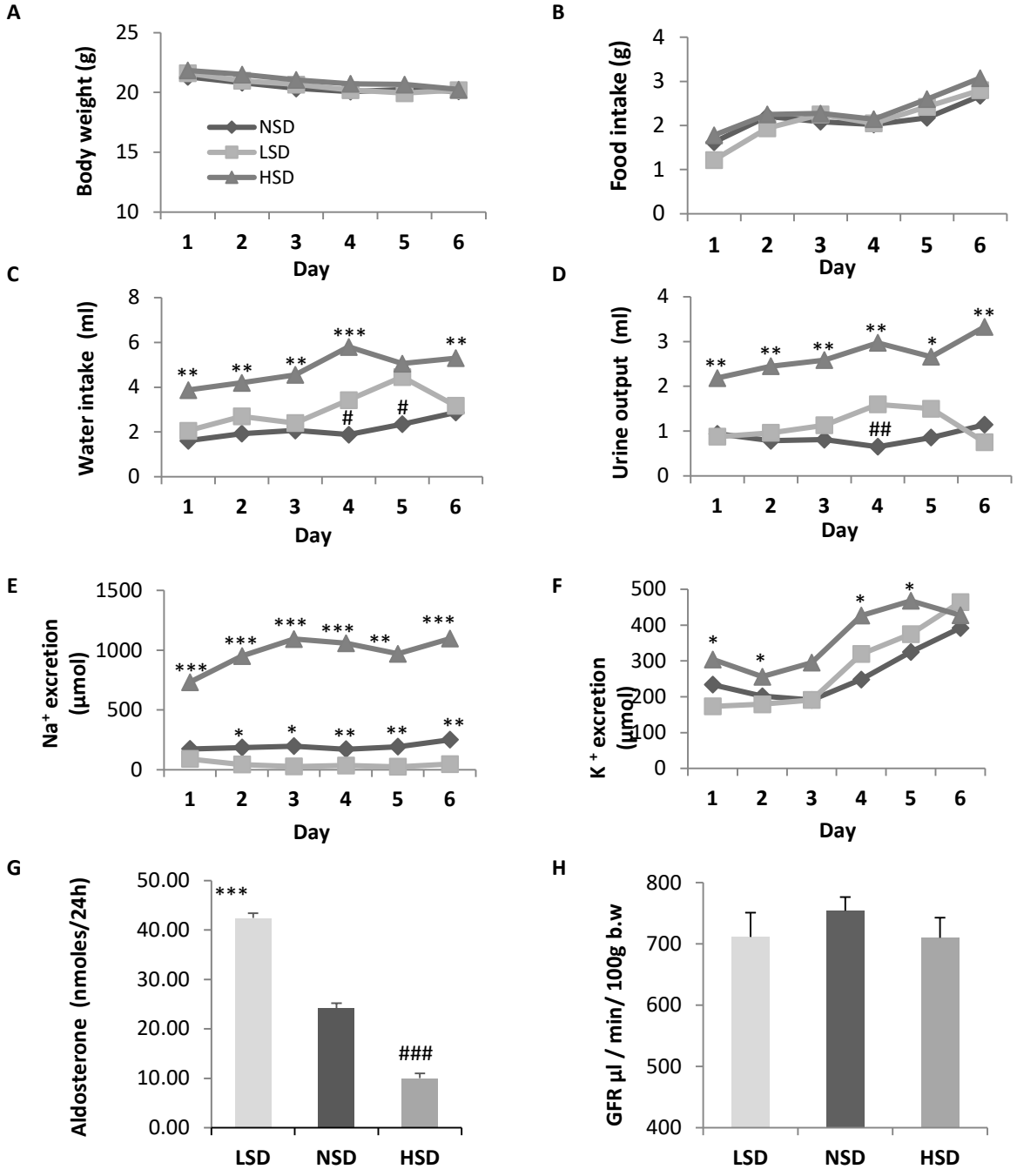
A
Body weight (g)
25
20
15
10
NSD
LSD
HSD
1 2 3 4 5 6
Day
B
Food intake (g)
4
3
2
1
0
1 2 3 4 5 6
Day
C
Water intake (ml)
8
6
4
2
0
** ** ** *** **
# #
1 2 3 4 5 6
Day
D
Urine output (ml)
4
3
2
1
0
** ** ** ** * **
##
1 2 3 4 5 6
Day
E
Na+ excretion (µmol)
1500
1000
500
0
*** *** *** *** ** ***
* * ** ** **
1 2 3 4 5 6
Day
F
K+ excretion (µmol)
500
400
300
200
100
0
* * * * *
1 2 3 4 5 6
Day
G
Aldosterone (nmoles/24h)
50.00
40.00
30.00
20.00
10.00
0.00
***
###
LSD NSD HSD
H
GFR µl / min/ 100g b.w
800
700
600
500
400
LSD NSD HSD

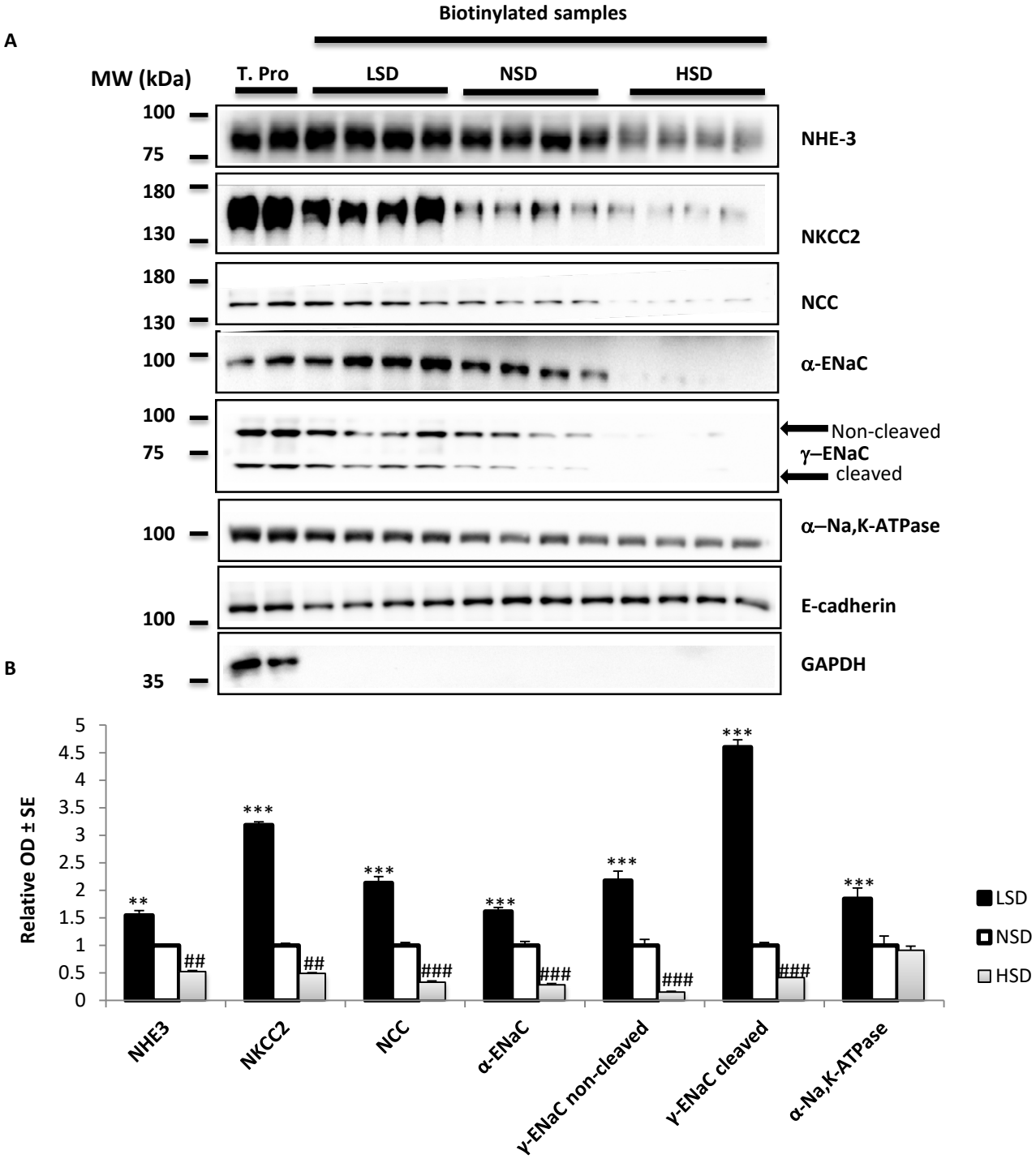
A
Biotinylated samples
MW (kDa)
T. Pro
LSD
NSD
HSD
100
75
180
130
180
130
100
100
75
100
100
35
NHE-3
NKCC2
NCC
α-ENaC
Non-cleaved
γ–ENaC
cleaved
α–Na,K-ATPase
E-cadherin
GAPDH
B
Relative OD ± SE
5
4.5
4
3.5
3
2.5
2
1.5
1
0.5
0
**
***
***
***
***
***
***
##
##
###
###
###
###
NHE3
NKCC2
NCC
α-ENaC
γ-ENaC non-cleaved
γ-ENaC cleaved
α-Na,K-ATPase
LSD
NSD
HSD

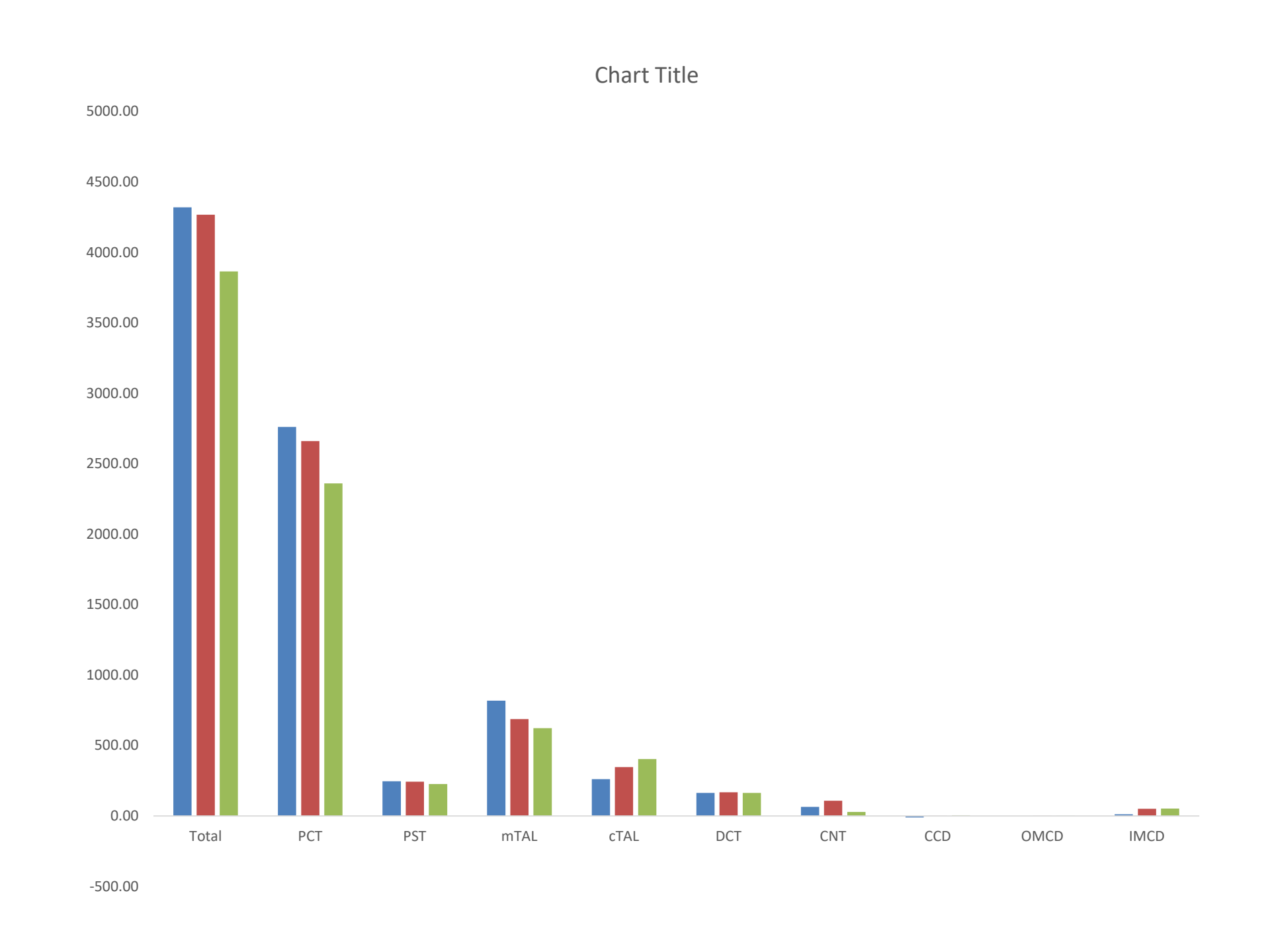
Chart Title
5000.00
4500.00
4000.00
3500.00
3000.00
2500.00
2000.00
1500.00
1000.00
500.00
0.00
-500.00
Total
PCT
PST
mTAL
cTAL
DCT
CNT
CCD
OMCD
IMCD

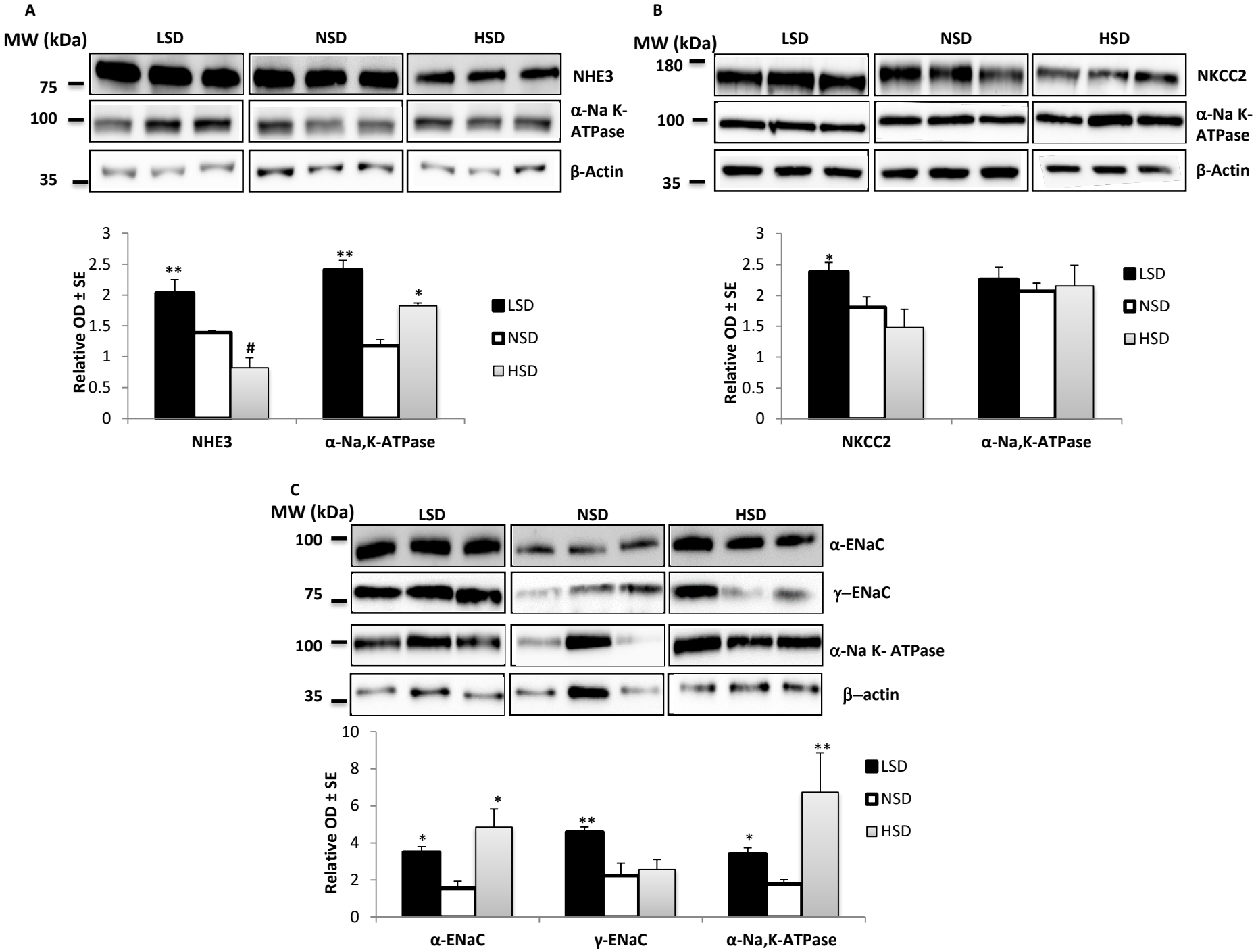
A
MW (kDa)
LSD
NSD
HSD
75
100
35
NHE3
α-Na K-ATPase
β-Actin
Relative OD ± SE
NHE3
α-Na,K-ATPase
B
MW (kDa)
180
100
35
NKCC2
α-Na K-ATPase
β-Actin
NKCC2
α-Na,K-ATPase
C
MW (kDa)
100
75
100
35
α-ENaC
γ–ENaC
α-Na K- ATPase
β–actin
α-ENaC
γ-ENaC
α-Na,K-ATPase

A

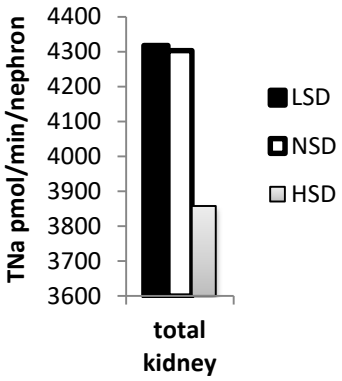
TNa pmol/min/nephron
4400
4300
4200
4100
4000
3900
3800
3700
3600
total kidney
LSD
NSD
HSD

B

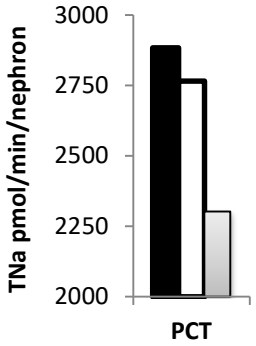
TNa pmol/min/nephron
3000
2750
2500
2250
2000
PCT

C

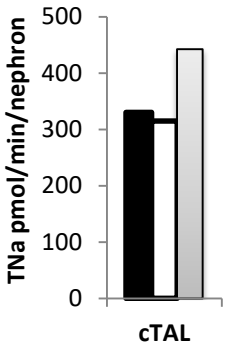
TNa pmol/min/nephron
500
400
300
200
100
0
cTAL

D

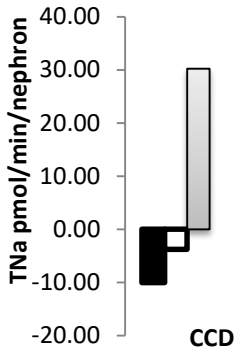
TNa pmol/min/nephron
40.00
30.00
20.00
10.00
0.00
-10.00
-20.00
CCD

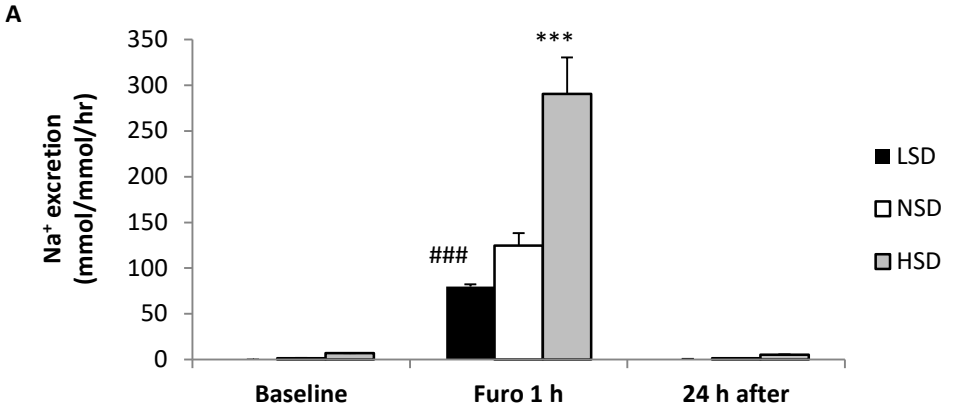
A
Na+ excretion (mmol/mmol/hr)
350
300
250
200
150
100
50
0
***
###
LSD
NSD
HSD
Baseline
Furo 1 h
24 h after

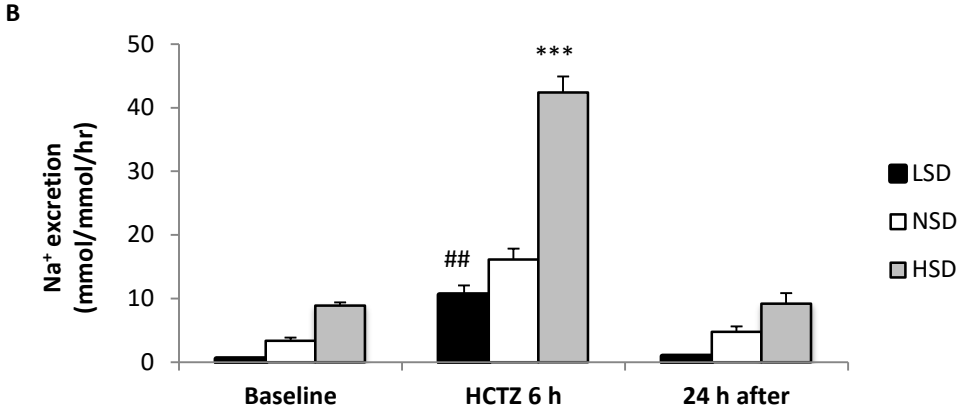
B
Na+ excretion (mmol/mmol/hr)
50
40
30
20
10
0
***
##
LSD
NSD
HSD
Baseline
HCTZ 6 h
24 h after

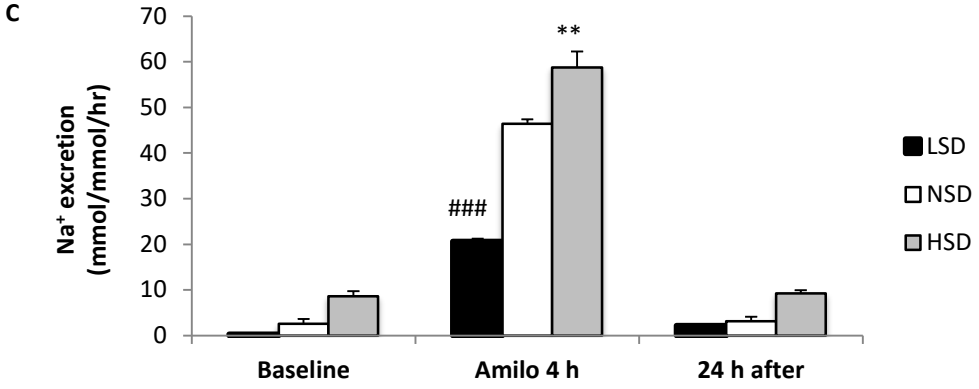
C
Na+ excretion (mmol/mmol/hr)
70
60
50
40
30
20
10
0
**
###
LSD
NSD
HSD
Baseline
Amilo 4 h
24 h after

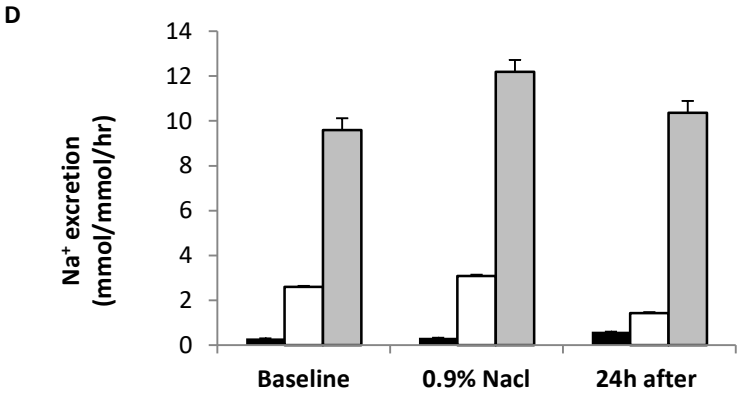
D
Na+ excretion (mmol/mmol/hr)
14
12
10
8
6
4
2
0
Baseline
0.9% Nacl
24h after

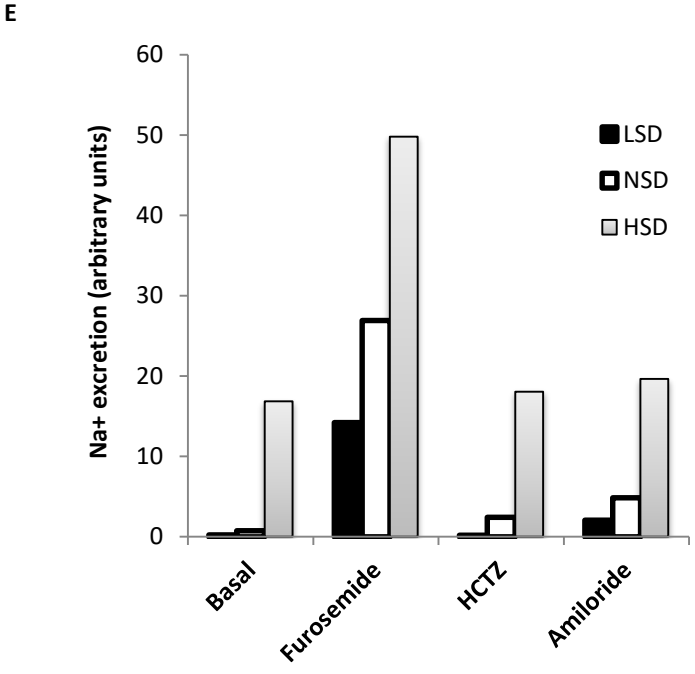
E
Na+ excretion (arbitrary units)
60
50
40
30
20
10
0
LSD
NSD
HSD
Basal
Furosemide
HCTZ
Amiloride

A

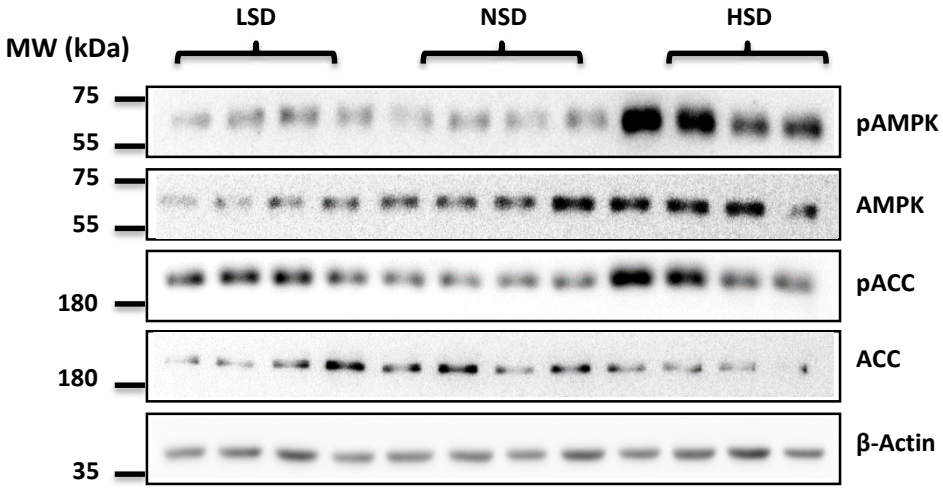
LSD
NSD
HSD
MW (kDa)
75
55
75
55
180
180
35
pAMPK
AMPK
pACC
ACC
β-Actin

B

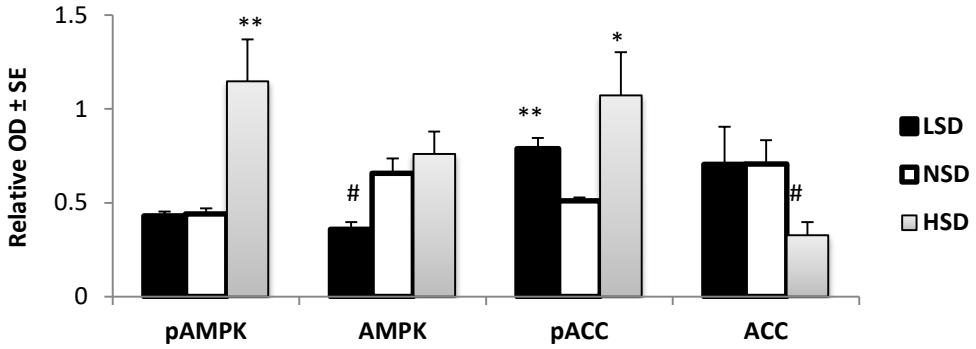
Relative OD ± SE
1.5
1
0.5
0
**
#
**
*
#
pAMPK
AMPK
pACC
ACC
LSD
NSD
HSD

A

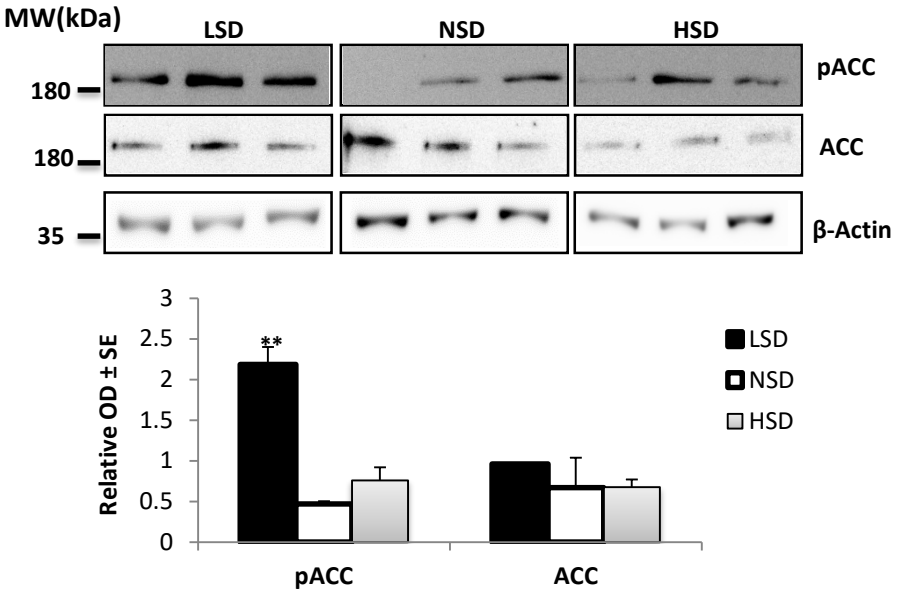
MW(kDa)
LSD
NSD
HSD
180
180
35
pACC
ACC
β-Actin
Relative OD ± SE
3
2.5
2
1.5
1
0.5
0
**
LSD
NSD
HSD
pACC
ACC

B

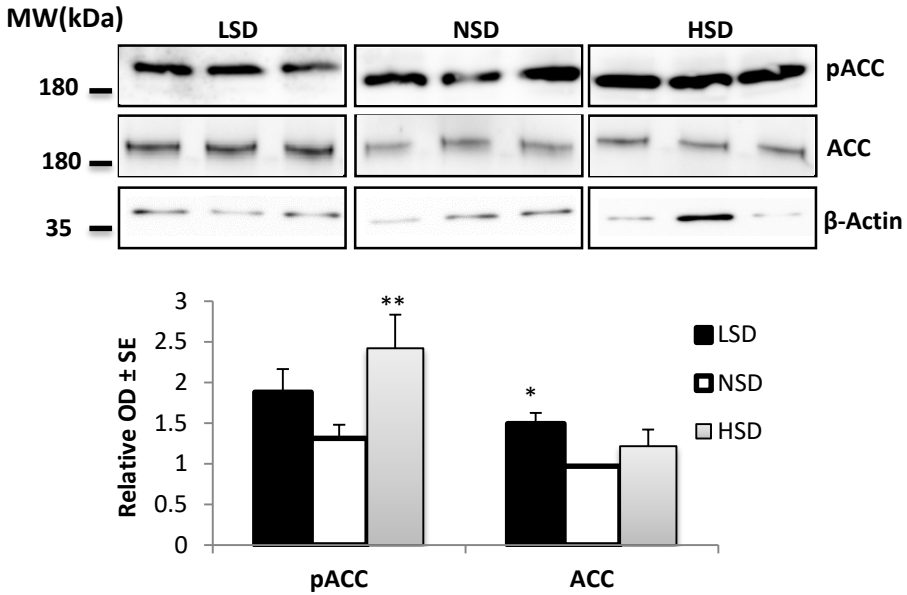
MW(kDa)
LSD
NSD
HSD
180
180
35
pACC
ACC
β-Actin
Relative OD ± SE
3
2.5
2
1.5
1
0.5
0
**
*
LSD
NSD
HSD
pACC
ACC

C

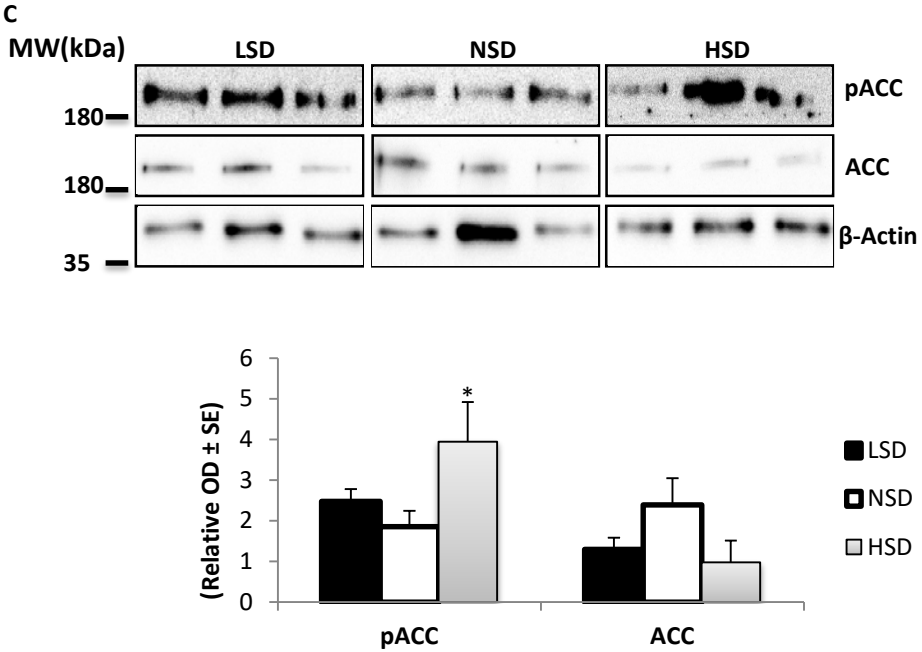
MW(kDa)
LSD
NSD
HSD
180
180
35
pACC
ACC
β-Actin
(Relative OD ± SE)
6
5
4
3
2
1
0
*
LSD
NSD
HSD
pACC
ACC

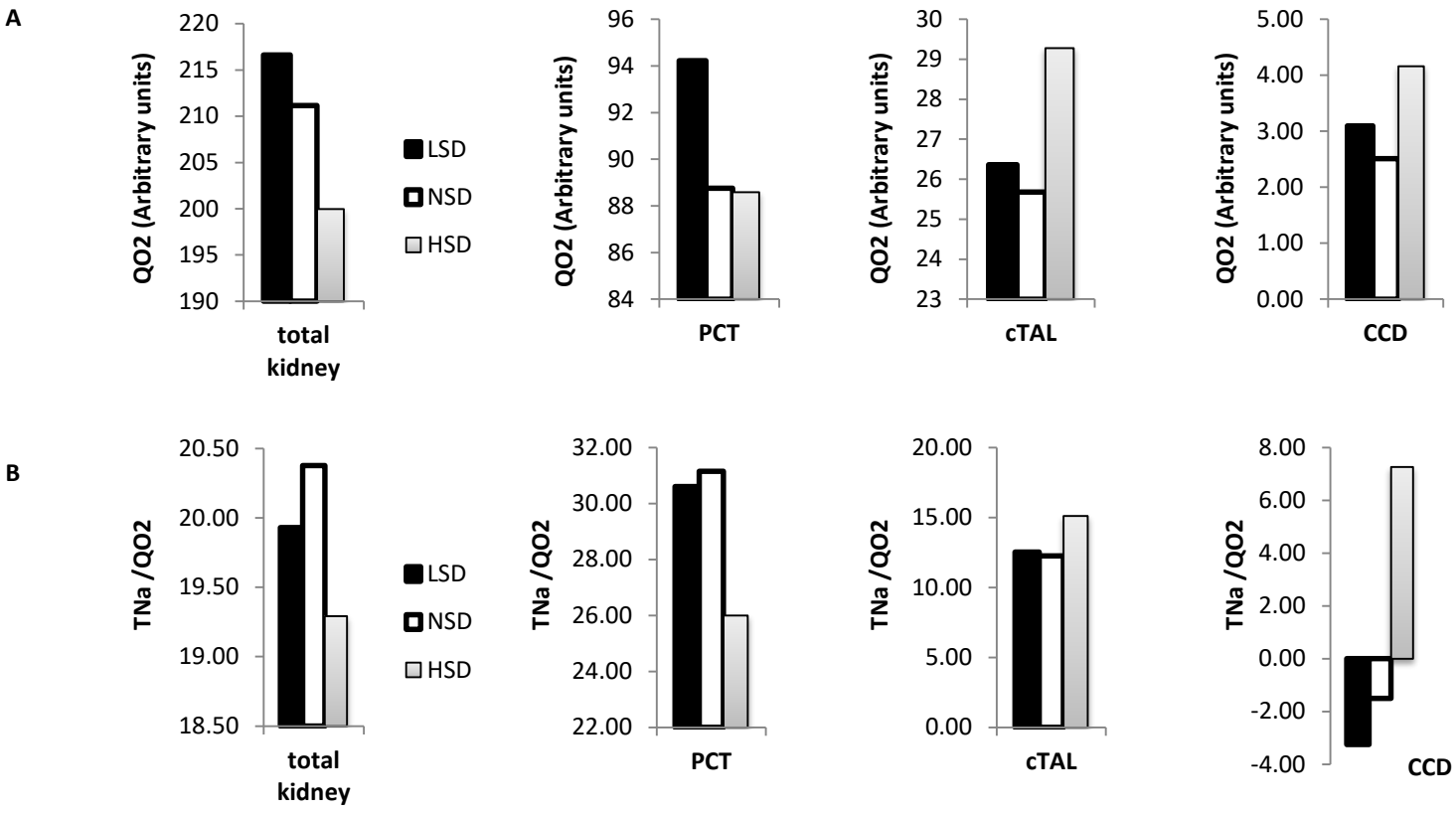
A
QO2 (Arbitrary units)
220
215
210
205
200
195
190
total kidney
LSD
NSD
HSD
96
94
92
90
88
86
84
PCT
30
29
28
27
26
25
24
23
cTAL
5.00
4.00
3.00
2.00
1.00
0.00
CCD
B
TNa /QO2
20.50
20.00
19.50
19.00
18.50
total kidney
32.00
30.00
28.00
26.00
24.00
22.00
PCT
20.00
15.00
10.00
5.00
0.00
cTAL
8.00
6.00
4.00
2.00
0.00
-2.00
-4.00
CCD

**Supplementary Table 1. Predicted vs. measured fractional changes in water and solute excretion.**

| | | LSD-to-NSD ratio | HSD-to-NSD ratio |
|---|---|---|---|
| $Na^+$ excretion | Experimental | 0.11 | 4.0 |
| | Model case 1 | 0.11 | 8.4 |
| | Model case 2 | 0.12 | 9.3 |
| $K^+$ excretion | Experimental | 0.71 | 1.2 |
| | Model case 1 | 0.20 | 1.5 |
| | Model case 2 | 0.21 | 1.7 |

Experimental results correspond to day 7 after the onset of the low- or high-salt diet.
Model case 1 accounts only for changes in transporter cell-surface expression (biotinylation results). Model case 2 also considers segment-specific changes in transporter expression. See text for details.

Fig. S1: Urinary chloride excretion

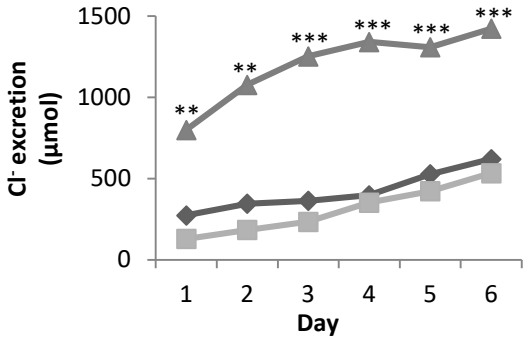

Fig. S2: $Na^+$ transporters abundance in total kidney extract under various $Na^+$ diet

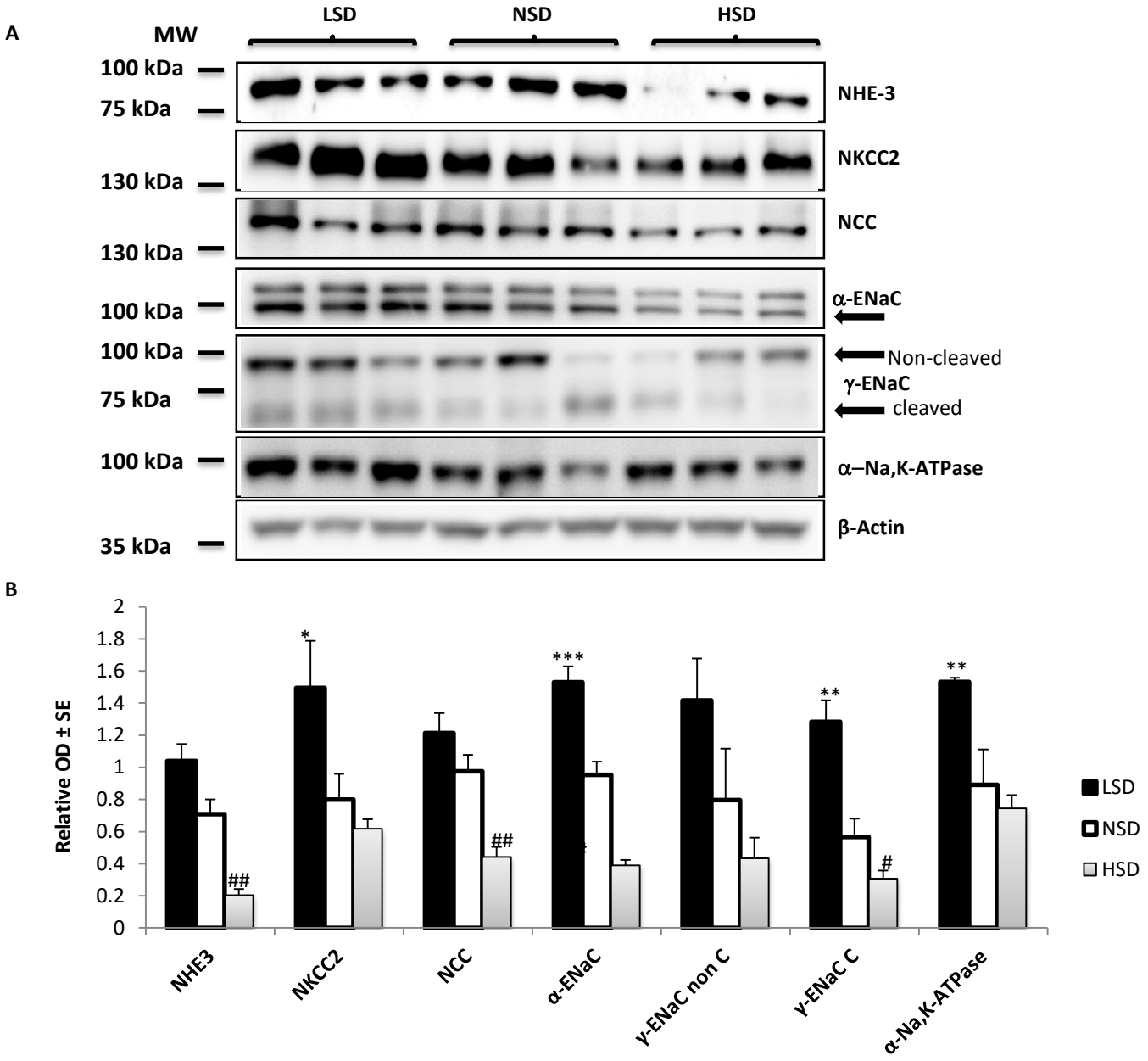

# Fig. S3: NCC phosphorylation in total kidney extract under various $Na^+$ diet

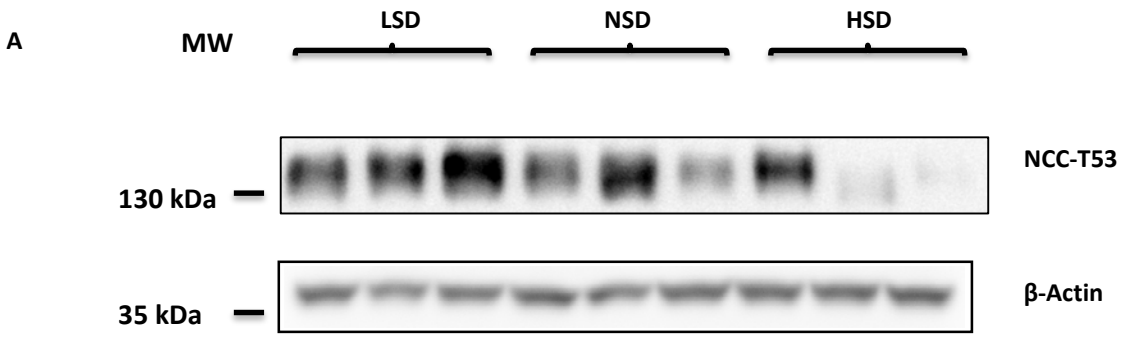


B

##  *

# Fig. S4: $H^+$_ATPase and pendrin abundance in total kidney extract under various $Na^+$ diet

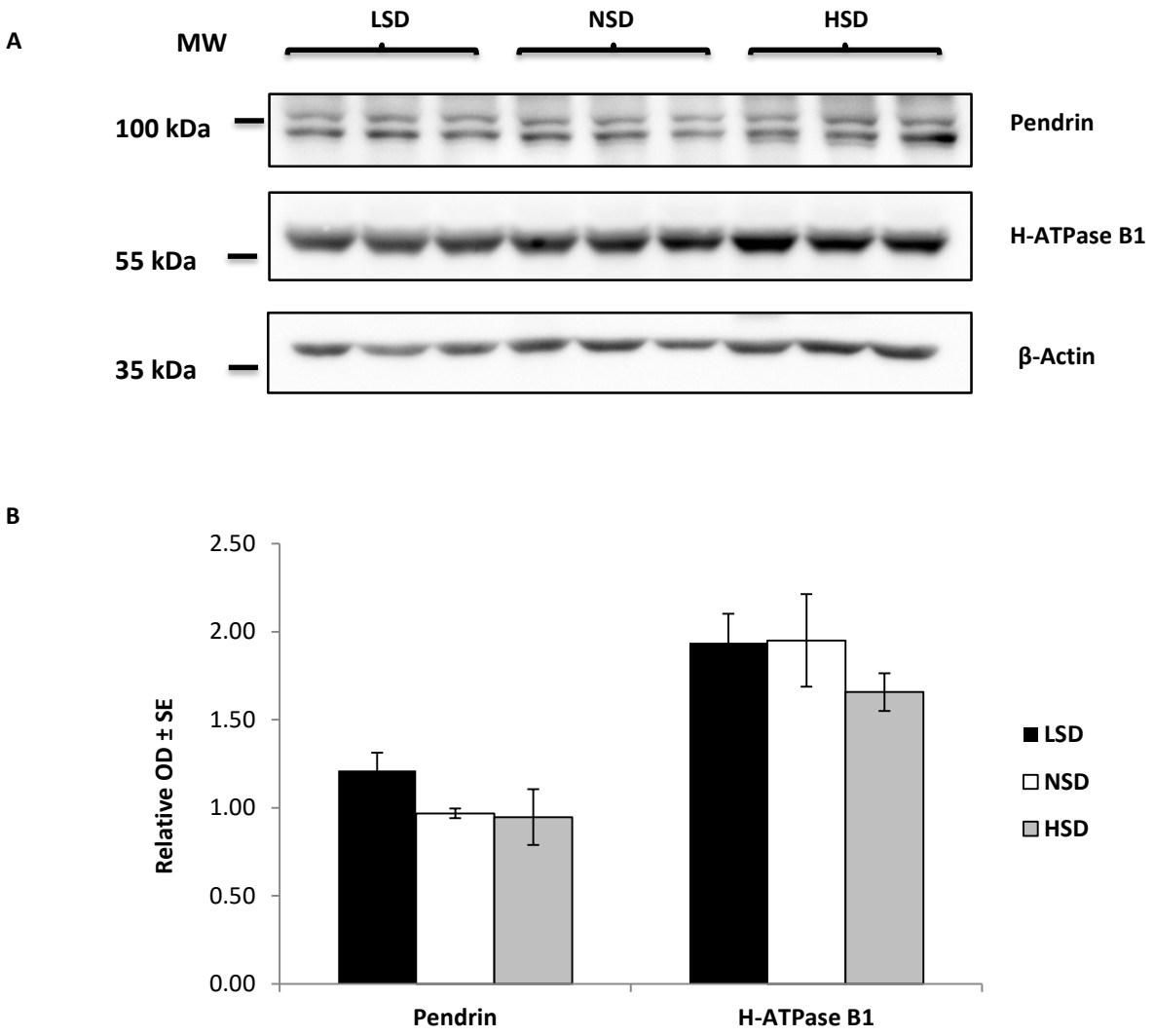

Fig. S5: Functional assessment of renal sodium transport in response to benzamil